Final Draft
of the original manuscript:

Liang, J.; Srinivasan, P.B.; Blawert, C.; Dietzel, W.:
Influence of chloride ion concentration on the electrochemical corrosion behaviour of plasma electrolytic oxidation coated AM50 magnesium alloy
In: Electrochimica Acta (2010) Elsevier

DOI: 10.1016/j.electacta.2010.05.087

Influence of chloride ion concentration on the electrochemical corrosion behaviour of plasma electrolytic oxidation coated AM50 magnesium alloy

J. Liang, P. Bala Srinivasan*, C. Blawert, W. Dietzel

Institute of Materials Research
GKSS-Forschungszentrum Geesthacht GmbH
D 21502 Geesthacht, Germany

*Corresponding Author (bala.srinivasan@gkss.de);
Phone: 00-49-4152-871997; Fax: 00-49-4152-871909

Key words

Magnesium alloy; Plasma electrolytic oxidation; Microstructure; Electrochemical corrosion; Chloride ion concentration; Degradation mechanism;

Abstract

The electrochemical degradation of a silicate- and a phosphate-based plasma electrolytic oxidation (PEO) coated AM50 magnesium alloy obtained using a pulsed DC power supply was investigated using potentiodynamic polarisation and electrochemical impedance spectroscopy (EIS) in NaCl solutions of different chloride ion concentrations viz., 0.01M, 0.1M, 0.5M and 1M. The surface of the PEO coated specimens after 50 h of immersion/EIS testing was examined by optical microscopy and scanning electron microscopy. The results showed that the corrosion deterioration of PEO coated magnesium alloy in NaCl solutions was significantly influenced by chloride ion concentration. The silicate-based coating was found to offer a superior corrosion resistance to the magnesium substrate than the phosphate based coatings in lower chloride ion concentration NaCl solutions (0.01 M and 0.1 M NaCl). On the other hand both these PEO coatings were found to be highly susceptible to localized damage, and could not provide an effective corrosion protection to Mg alloy substrate in solutions containing higher chloride concentrations (0.5 M and 1 M). The extent of localized damage was observed to be more with increase in chloride concentration in both the cases.

1. Introduction

Owing to the high strength to weight ratio, good dimensional stability, electromagnetic shielding and damping characteristics and good recyclability, magnesium alloys are now contemplated for a wide range of industrial applications **[1,2]**. However, a critical limitation for the extensive usage of magnesium alloys is their high susceptibility to corrosion, especially in aggressive environments, which is primarily attributed to the high chemical activity of magnesium and the unstable passive film on the surface of these alloys **[3-5]**. Many researchers have addressed the influence of various corrosive environments on the corrosion behaviour of pure magnesium and/or magnesium alloys for the understanding of environmental factors controlling corrosion **[5-12]**. It was found that even small amounts of chloride ions in

aqueous solution can break the naturally formed passive film and lead to localized corrosion of magnesium alloys and the corrosion rate was reported to increase with increasing chloride ion concentration in the environment [3].

Many attempts have been made to overcome the corrosion problems of magnesium and its alloys. These include the control of impurities, alloying, rapid solidification and application of suitable protective coatings [13]. Among these techniques, the protection through proper surface modification seems to be one of the most effective methods for corrosion prevention of magnesium alloys. Various treatments, such as plating, conversion coatings, anodizing, gas-phase deposition, laser surface alloying and polymer coatings, have been attempted in recent times, amidst which the plasma electrolytic oxidation (PEO) process has been popular since 2000 [13-16]. A relatively thick and hard ceramic/oxide coating can be produced by the PEO process on the surface of magnesium alloys to improve their corrosion and wear resistance remarkably [14-18].

Even though PEO of magnesium alloys can be accomplished in many different electrolytes, silicate and phosphate based electrolytes are the most widely employed electrolytes even today [19-24]. In our previous work [21], the electrochemical behaviour of PEO coated AM50 magnesium alloy produced from silicate and phosphate electrolytes in 0.1 M NaCl solution was reported. It was found that the corrosion resistance of the PEO coating formed in the silicate electrolyte was superior to that formed from the phosphate electrolyte, which was related to the microstructure and composition of the PEO coatings. This paper is an extended study of the above cited work, in order to assess the corrosion behaviour of the aforementioned PEO coated AM50 magnesium alloy. The scope of this work is to investigate the influence of chloride ion concentration on the electrochemical degradation behaviour of these coatings and to understand the underneath corrosion mechanisms.

2. Experimental

AM50 magnesium alloy specimens of size 15 mm × 15 mm × 4 mm with a mass fraction of 4.4% ~ 5.5% Al, 0.26% ~ 0.6% Mn, max 0.22% Zn, max 0.1% Si, and Mg balance were used as the substrate in this investigation. The specimens were ground with 500, 800, 1200 and 2500 grit emery sheets and cleaned with ethanol before the PEO treatment.

The plasma electrolytic oxidation treatment was carried out using a pulsed DC power source with a pulse ratio of t_{on} : t_{off} = 2 ms : 20 ms in alkaline silicate electrolyte and phosphate electrolytes. The silicate electrolyte contained Na_2SiO_3 (10.0 g/l) and KOH (1.0g/l) in distilled water and the phosphate electrolyte was constituted with Na_3PO_4 (10.0 g/l) and KOH (1.0 g/l) in distilled water. Coatings were produced at a constant current density of 15 $mA{\cdot}cm^{-2}$ for 30 minutes in both the electrolytes. In all the cases, the temperature of the electrolyte was always kept at 10 ± 2˚C by a water cooling system. All the coated specimens were rinsed thoroughly in distilled water and dried in ambient air immediately after the PEO treatment. Roughness measurements were made in a Hommel profilometer to assess the mean surface roughness (R_a) of the coated surfaces.

Electrochemical tests were carried out using a Gill AC potentiostat/frequency response analyser system to evaluate the corrosion behaviour of uncoated and PEO coated specimens. A typical three electrode cell, with a saturated Ag/AgCl (saturated with KCl) as reference electrode, a platinum mesh counter electrode and the PEO coated specimen as the working electrode (0.5 cm^2 exposed area) was used. The electrochemical tests were conducted in NaCl solutions with chloride ion concentrations of 0.01 M, 0.1 M, 0.5 M and 1 M, respectively. All the solutions prepared from deionized water and sodium chloride (analytically pure) were nearly neutral with pH of around 6.8 ± 0.2. Potentiodynamic polarisation tests were performed at a scan rate of 0.5 $mV \cdot s^{-1}$ to a final anodic current density of 0.1 $mA \cdot cm^{-2}$ after an initial 0.5 h exposure to the test electrolyte for achieving a stabilized open circuit potential. Electrochemical impedance spectroscopy (EIS) studies were performed at open circuit potential with an AC amplitude of 10 mV over the frequency range of 30,000 Hz to 0.01 Hz on specimens exposed to the corrosive electrolyte for different durations viz., 0.5, 2, 5, 10, 25 and 50 h to understand the degradation phenomena. All the electrochemical tests were performed at room temperature, i.e., 21 ± 1°C and the tests were performed in triplicate to ascertain reproducibility.

Macroscopic examination to assess the morphology of the corroded surface of the specimens after the EIS tests was performed in a stereo-zoom optical microscope and in a Cambridge Stereoscan 250 scanning electron microscope. UTHSCSA® ImageTool was employed for the assessment of the area fraction of corrosion damaged regions in the specimens subjected to EIS tests for 50 h.

3. Results and Discussion

3.1 Microstructure and composition

In our previous work **[21]**, the phase composition and microstructure of the PEO coatings prepared from the Si- and P-based electrolytes were analyzed and documented. X-ray diffraction (XRD) analyses indicated that the PEO coating produced in silicate electrolyte (Si-PEO) was composed predominantly of Mg_2SiO_4 and MgO, whilst the PEO coating formed in phosphate electrolyte (P-PEO) was constituted with $Mg_3(PO_4)_2$ and MgO. According to the relative intensity of the peaks in XRD, it was observed that Mg_2SiO_4 was the main phase in the Si-PEO coating, whilst the MgO phase dominated in the P-PEO coating.

The surface and cross-section morphologies of the Si-PEO and P-PEO coating are shown in **Fig. 1**. SEM observations revealed that the Si-PEO coated surface had a larger number of uniformly distributed pores of 5 – 15 μm size (Fig. 1a), whilst in the P-PEO coating the pores were much less in number but larger in size (10 – 30 μm in diameter) (Fig. 1b). The roughness (R_a) of the Si-PEO and P-PEO coatings were 1.0 ± 0.2 μm and 3.2 ± 0.2 μm, respectively. It can be seen that the cross-section of the Si-PEO coating contained many pores and other irregular defects, which were not inter-connecting each other (Fig. 1c). While in the cross-section of the P-PEO coating, through-going pores into the inner sections of the coating was observed, though most of other parts was less defective (Fig. 1d). A closer look at the cross-section of the

specimens showed that the Si-PEO coating had a very thin interface region at the bottom of coating with low defect levels. However, in the P-PEO coating, the interface region was relatively thicker and had numerous defects. Arrabal et al. [25] observed a similar microstructural characteristics in the phosphate based PEO coating on a Mg alloy substrate. The thickness of the Si-PEO and P-PEO coatings obtained in a 30 min treatment were 17 ± 3 μm and 25 ± 2 μm, respectively.

3.2 Polarisation behaviour

The corrosion behaviour of Si-PEO and P-PEO coated specimens evaluated by potentiodynamic polarisation after 0.5 h of exposure in NaCl solutions of different chloride ion concentrations are presented in **Fig. 2a** and **Fig. 2b,** respectively. The corrosion potential (E_{corr}), corrosion current density (i_{corr}) and the breakdown potential (E_{bd}) derived from potentiodynamic polarisation plots are summarized in **Table 1** and **Table 2**, respectively. From Table 1, it can be seen that the i_{corr} values of Si-PEO coated specimens were in the same order of magnitude in 0.01 M and 0.1 M NaCl solutions, whilst the i_{corr} values increased by nearly two orders of magnitude when the Si-PEO coated specimens were exposed to 0.5 M and 1 M NaCl solutions. It was also found that the Si-PEO coated specimen exposed in 0.01 M NaCl registered breakdown potentials of -685 ± 150 mV vs. Ag/AgCl, whilst the specimen in 0.1 M NaCl showed more active breakdown potentials (-1150 ± 40 mV vs. Ag/AgCl). On the other hand, the Si-PEO coating in 0.5 M and 1 M NaCl solutions showed breakdown at the corrosion potential itself, as was evidenced by the rapid increase in current density in the anodic region of the polarisation plots.

When the P-PEO coated specimens were immersed in NaCl solutions of different chloride ion concentrations, the change of the i_{corr} values was found to exhibit a similar trend as that observed for Si-PEO coated specimens. The P-PEO coated specimen exposed to 0.01 M NaCl solution registered a breakdown potential of -1325 ± 15 mV vs. Ag/AgCl, which was more positive than that in 0.1 M NaCl solution (-1390 ± 10 mV vs. Ag/AgCl). While in 0.5 M NaCl solution, the observed breakdown potential of around -1480 mV vs. Ag/AgCl was close to its corrosion potential, the P-PEO coating broke-down at the corrosion potential itself in 1 M NaCl solution.

Generally, the breakdown potential (E_{bd}) of coated alloys in corrosive environments is considered as an indication of the capability of a coating to resist localized corrosion damage [26,27]. The breakdown of the coating through the defective sites, would expose the underneath substrate to the corrosive environment. Therefore, a more positive breakdown potential of the coated alloy implies that the coating is more stable in terms of its localized corrosion performance. From the E_{bd} values in Table 1 and Table 2, it can be seen that the Si-PEO coated specimens exhibited much higher positive breakdown potential than the P-PEO coated specimens in lower chloride ion concentration solutions viz., 0.01 M and 0.1 M NaCl, which signified that the Si-PEO coating was more stable against breakdown and has better localized corrosion performance than the P-PEO coating, despite the fact that this

coating was relatively thinner. Considering the characteristics of the porous structure of the PEO coatings, the observed breakdown potential of PEO coating also suggested that not all the pores were inter-connected and/or penetrated through the cross-section of the coating to reach the coating-substrate interface. Nevertheless, when the PEO coated specimens were exposed to more aggressive corrosive environments viz., 0.5 M and 1 M NaCl solutions, the breakdown potentials were close to or at their respective corrosion potentials, which brought out the strong influence of chloride ion concentration on the susceptibility of the coatings to localized damage.

3.3 EIS characteristics

The corrosion deterioration of PEO coated specimens in corrosive electrolytes with prolonged immersion time up to 50 h was examined by EIS measurements. The EIS spectra (Nyquist plots) of Si-PEO and P-PEO coated specimens obtained in 0.01 M NaCl solution are presented in **Fig. 3a** and **3b,** respectively. For the Si-PEO coating, EIS tests up to 25 h of immersion times showed a very large near-linear impedance locus. The test after 50 h of immersion resulted in a Nyquist plot with partially resolved capacitive loop, with a slightly depressed locus. Nevertheless, the Si-PEO coating had offered an excellent resistance even after 50 h of immersion as can be observed in Figure 3a. The behaviour of the P-PEO coating in 0.01 M NaCl solution was little different from that of the Si-PEO coating. All the Nyquist plots, obtained after different times of exposures to the electrolyte, showed capacitive loops. The resistance offered by this coating was substantially lower than that of the Si-PEO coating at all exposure times.

In 0.1 M NaCl solution, Nyquist posts of Si-PEO coated specimen were found to exhibit a partially-resolved capacitive loop in the tests performed after 0.5, 2 and 5 h of immersion (Fig. 4a). The resistance values were high in the all the above conditions, and appear to be the same, indicating that the coating did not undergo any significant degradation. However, after 10 h of exposure, the resistance dropped substantially, and with further exposure up to 25 and 50 h, a further degradation was observed. On the other hand, the P-PEO coating was found to show a much lower resistance values, at all the test durations compared to its Si-PEO counterpart. Further, the degradation of the P-PEO coating appears to be quicker when compared to that of the Si-PEO coating, as can be observed from **Figs. 4a** and **4b**, respectively. The emergency of an inductive loop in Nyquist plot of the P-PEO coated specimen in the EIS test after 50 h of immersion signified the localized corrosion damage of underneath Mg alloy substrate **[28]**.

The degradation of both the PEO coatings was found to be accelerated by the increase in chloride ion concentration in the corrosive environment. The EIS behaviour of the coated specimens in 0.5 M and 1 M NaCl solutions after different durations of exposures are depicted in **Figs. 5** and **6**, respectively. In both these aggressive electrolytes, the inductive loop appeared in the EIS tests after 5 h of exposure for both the coated specimens.

3.4 Morphology of corroded surfaces

The examination of the corroded surfaces after 50 h of exposure/EIS testing in NaCl solutions of different concentrations revealed the differences in the extent of corrosion damage of the Si-PEO and P-PEO coated specimens. **Fig. 7** presents the macroscopic appearance of corroded surface after 50 h of testing in different corrosive electrolytes and **Fig. 8** shows the scanning electron micrographs of corroded area corresponding to the specimens/regions labeled in Fig. 7. The SEM surface morphologies of as-coated PEO specimens are also presented in Fig. 8 for comparison purposes. It can be seen that the Si-PEO coated specimen has no observable corrosion damage after 50 h immersion/EIS testing in 0.01 M NaCl solution. The SEM micrographs depicted in Figs. 8a and 8b reveal that the surface in the exposed area did not undergo any major changes when compared to the as-coated surface. There was also no macroscopic damage on the P-PEO coated surface after 50 h of immersion/EIS testing in 0.01 M NaCl solution (Fig. 7 and Fig. 8c). However, the higher magnification SEM micrograph shown in Fig. 8d revealed slight corrosion damages in the pores of the coating (marked by arrows). In 0.1 M NaCl solution, too, there was no observable damage on the Si-PEO coating surface after 50 h of immersion (Fig. 7 and Fig. 8e). The higher magnification SEM micrograph (Fig. 8f) also demonstrated that the coating surface did not suffer from any significant corrosion degradation, but it seemed that a slight dissolution had occurred at the pores. In the case of the P-PEO coated specimen, however, the corrosion damage was evident in the macroscopic morphology in Fig. 7, in which localized corrosion damage was observed on the corroded surface, as represented in Fig. 8g. The higher magnification micrograph shown in Fig. 8h indicated that the other regions of the coating in exposed area also suffered from corrosion degradation and the corrosion degradation was confined mostly to the pores. Much different from the morphologies of as-coated surface, the pores in P-PEO coating were damaged and seemed to be filled with corrosion products after 50 h of immersion/EIS testing in 0.1 M NaCl solution. When the PEO coated specimens (Si-PEO and P-PEO) were exposed to 0.5 M NaCl solution and subjected to EIS tests after 50 h, localized corrosion damages were clearly observed on the surface of both these specimens. The percentage of corrosion damage area in whole exposed area measured by UTHSCSA® ImageTool was 5±1% and 8±2%, respectively, for the Si-PEO and P-PEO coated specimens. The SEM micrographs depicted in Figs. 8i and k showed that these damaged regions were filled with corrosion products. Regions outside the localized damage in the surface exposed to the electrolyte suffered a corrosion damage only confining to the pores, the extent of which was higher than that observed for the respective specimens in 0.01 M and 0.1 M NaCl solutions (Fig. 8j and l). With the chloride ion concentration increasing further up to 1 M, it was observed that the localized corrosion damages in the Si-PEO and P-PEO coated specimens were more severe and larger than those in 0.5 M NaCl solution. The corroded surface area assessment showed that the damage was around 18±2% and 16±2% in the Si-PEO and P-PEO coated specimens, respectively. The corrosion damage in the rest of the exposed area in these specimens are shown in Fig. 8n and p, and the morphological features were similar to those observed in the specimens tested in 0.5 M NaCl solution.

3.5 Degradation mechanisms

In addition to providing quantitative corrosion behaviour, the EIS tests can provide detailed information on the corrosion process at the electrolyte/ electrode interface and the property changes of the electrode, which is very important to understand the corrosion mechanism of the coating systems **[29]**. Taking into account the microstructural characteristics and the EIS behaviour of the PEO coated specimens, the schematic representations of the coatings and the corresponding equivalent circuits for fitting the EIS data (Figs. 3-6) of Si-PEO and P-PEO coatings are proposed in **Fig. 9** and **Fig. 10**, respectively. The equivalent circuits were established based on a reasonable fitting of the experimental values and a good description of the measured system by keeping the number of circuit elements to suit the cross-section morphology of the coatings. The elements in these equivalent circuits include R_s (the electrolyte resistance), R_1 (resistance of the porous layer/coating, more specifically the resistance of the defects, like pores/cracks of the PEO coating or the layer of corrosion products after localized corrosion initiated) paralleled with CPE_1 (a constant phase element representing the dispersion of porous coating/layer capacitance), R_2 (resistance of the compact layer including that of the coating/substrate interface) paralleled with constant phase element CPE_2, Z_w (a Warburg component associated with the diffusion of charged electrolyte across the PEO coating because of the presence of concentration gradient in the PEO coating during immersion process), L (inductance associated with relaxation processes involving the dissolution of metal to ions leading to the formation of corrosion products and the adsorption of electrolyte-active species at the defective sites), and R_L (inductive resistance of adsorption of species at localized defective sites) **[23,29-32]**. In these equivalent circuits, Fig. 9a was appropriate to fit the EIS data of Si-PEO coated specimens in shorter immersion durations (up to 10 h in 0.01 M NaCl solution, up to 5 h in 0.1 M NaCl solution, only 0.5 h in 0.5 M and 1 M NaCl solutions), because the penetration of corrosive electrolyte into the coating was slow and this non-homogeneous diffusion process has brought in the diffusion characteristic (Warburg impedance) EIS spectra. An electrochemical equivalent circuit as shown in Fig. 9b was employed to fit the EIS spectra of Si-PEO coated specimen when the concentration gradient of corrosive electrolyte in the coating vanished after sufficient time of immersion and a circuit as given in Fig. 9c was used to fit the EIS spectra of Si-PEO coated specimen after the initiation of localized corrosion, evinced by the inductive loop in the Nyquist plots. On the other hand, Fig. 10a and b were used for fitting the EIS spectra of P-PEO coated specimen before and after localized corrosion initiation, respectively. To evaluate the corrosion deterioration behaviour of PEO coated magnesium alloy, the change in the resistances R_1 and R_2 corresponding to Si-PEO and P-PEO coated specimens with progressive immersion time was represented in **Fig. 11** and **Fig. 12**, respectively.

In dilute NaCl solution (0.01 M NaCl), according to the change of fitting values of R_1 and R_2 in Fig. 11a and b, high and stable corrosion resistances of the Si-PEO coating were registered during 0.5 – 10 h immersion process, which meant that the Si-PEO coating has no pronounced deterioration in this

condition. At this immersion stage, because the pores and defects were not inter-connecting and chloride ion concentration in 0.01 M NaCl solution was low, the corrosive electrolyte permeated slowly into the PEO coating through these intrinsic defects. In the EIS spectra, this non-homogeneous diffusion process of corrosive electrolyte in PEO coating was reflected as Warburg response. With prolonged immersion time (25 – 50 h), both R_1 (the porous coating resistance) and R_2 (the compact layer/coating-substrate interface resistance) were found to decrease slightly. While the slight decrease of R_1 after 10 h of immersion is attributed to the permeation of more corrosive electrolyte into the defects (pores and/or cracks) in longer immersion process, the decrease of R_2 is ascribed to the degradation of PEO coating itself, because the MgO phase in the Si-PEO coating is not thermodynamically stable in aqueous solutions and is vulnerable to hydration to form $Mg(OH)_2$ **[33,34]**. With the degradation of MgO in the coating, new defects could be formed in the compact layer and also at the coating/substrate interface. At the same time, the diffusion process weakened (at 25 h of immersion) and finally disappeared after 50 h of immersion. However, the high resistance value R_1 of the order 10^2 kΩ·cm² suggests clearly that the degradation of the coating in the form of dissolution of MgO phase was insignificant in 0.01M NaCl solution.

When the P-PEO coated specimen was immersed in the 0.01 M NaCl solution, it can be seen from Fig. 12 that both R_1 and R_2 began to drop rapidly to lower values with the increase in immersion time from 0.5 h to 10 h. The drop in resistance R_1 is more significant and prominent that R_2. The quick decrease of R_1 and R_2 was obviously related to the through-going pores into the inner sections in P-PEO coating, making the permeation of corrosive electrolyte into the coating easier and faster. The capacitive loops observed in the EIS spectra (Fig. 3b) suggests clearly the absence of diffusion process. With prolonged immersion process (over 10 h), the resistance R_1 decreased to very low values. However, the resistance R_2 was found not to deteriorate, but was increased slightly in the 25 h and 50 h exposures. The reason for amelioration of R_2 is that more intense corrosion degradation (hydration process) was possible for the MgO, the main composition in the P-PEO coating, when it was saturated with corrosive electrolyte. With the hydration of MgO, the newly formed $Mg(OH)_2$ partially blocked the defects (pores and/or cracks), because the molar volume of $Mg(OH)_2$ is larger than that of MgO and could serve as protective barrier to corrosive electrolyte, hence increasing the corrosion resistance of PEO coating after 10 h of immersion **[23,33]**. It should be emphasized that the high resistance (R_2) values of the Si-PEO and P-PEO coatings comes through different mechanisms. Whilst in the former case, the stability of the coatings is from the predominant magnesium silicate phase of the coating and the slight drop in resistance observed after 50 h of immersion is due to the dissolution of MgO phase in this coating, which is present in small amounts, in the latter case, hydration of MgO leading formation of $Mg(OH)_2$ provided a barrier effect with a high resistance also resisting the localized damage. It is to be pointed out that the chloride ion concentration in 0.01 M NaCl solution is very low, which is not aggressive enough to damage the $Mg(OH)_2$ barrier and to activate the underneath Mg alloy substrate to initiate the localized corrosion quickly **[14]**. In order to ascertain this, the uncoated AM50 Mg alloy substrate was subjected to EIS tests in 0.01 M NaCl solution.

The Nyquist plots shown in **Fig. 13a** clearly reveal that no localized corrosion was observed in 50 h immersion tests, which corroborates the above observations/EIS discussions pertaining to the P-PEO coated substrate. When compared the corrosion resistance of these two PEO coated specimens, it can be seen that the Si-PEO coated specimen showed consistently higher R_2 in 0.01 M NaCl solution at all exposure durations (EIS tests) than the P-PEO coated specimen. This is mainly ascribed to the relatively smaller pore sizes and denser Si-PEO coating.

When the Si-PEO coated specimen was exposed to 0.1 M NaCl solution, a relatively lower R_1, but nearly the same R_2 as those observed in 0.01 M NaCl solution were recorded during 0.5 – 5 h immersion. After 5 h of immersion, the resistance R_2 dropped with immersion time, suggesting evident corrosion deterioration of the PEO coating. The formation of corrosion products and the filling of the pores (Fig. 8f) suggest the deterioration of the coating in this electrolyte. Nevertheless, the coating did not undergo any localized damage, as evidenced by the corroded surface examination (Fig. 7 and Fig. 8e). In the case of P-PEO coated specimen, the corrosion deterioration trend (changes of R_1 and R_2) in 0.1 M NaCl solution was similar to that in 0.01 M NaCl solution during 0.5 – 10 h immersion process (Fig. 12a and 12b). With prolonged immersion time (over 10 h immersion), however, the resistance R_2 was found to decrease greatly, which was different from that of P-PEO coated specimen in 0.01 M NaCl solution. It was due to fact that the hydrated products $Mg(OH)_2$ from MgO could not provide the blocking effects as it was more easily degraded further in 0.1 M NaCl solution **[9]**. This had led to the transport of corrosive electrolyte through the defects on to the underneath Mg substrate, which induced the localized corrosion damage the Mg substrate in the prolonged immersion viz., beyond 10 h.

With the initiation of localized corrosion of underneath Mg alloy substrate, the corrosion products formed at the coating/substrate interface grew to such a level that it exerted a stress which could lift/damage the PEO coating **[21]**. The damage of the PEO coating in these sites resulted in further exposure of the underneath Mg alloy substrate and this has further led to more severe corrosion process. As a result, the fitting values of R_1 (referring to the corrosion products layer resistance after localized corrosion initiated) and R_2 (representing charge transfer resistance of the Mg alloy substrate after localized corrosion initiated) decreased drastically. At the same time, owing to the localized corrosion attack at these defective sites, the corrosion deterioration in the rest of the exposed area was retarded. In this way, a localized damage appeared on the specimen surface (Fig. 8g) after 50 h immersion process. The above observations are substantiated by the assessment of uncoated AM50 Mg alloy substrate in 0.1 M NaCl solution. It is clear from **Fig. 13b** that the magnesium substrate underwent localized damage in the EIS tests after 10 h of immersion, evidenced by the inductive loop in the Nyquist plots. The resistance offered by the P-PEO coating could only defer the onset of localized damage to 50 h, and could not prevent if fully.

In more concentrated NaCl solutions (0.5 M and 1 M NaCl), the changes of R_1 (resistance of the porous regions of the coating) and R_2 (resistance of the

compact layer and coating/substrate interface) of Si-PEO coated specimens with immersion time was very quick when compared to those in lower concentration NaCl solutions (0.01 M and 0.1 M NaCl). The observation that the R_1 and R_2 were much inferior to those in lower chloride ion concentration solutions at the initial 0.5 h immersion test (Fig. 11a and b) is consistent with the results of polarisation tests. As the Si-PEO coating was susceptible to breakdown in higher chloride ion concentration solutions, corrosive electrolyte could easily ingress into the underneath Mg alloy substrate. The localized damage was evident after 5 h of immersion in 0.5 M NaCl solution and after 2 h of immersion in 1 M NaCl solution as manifested by the emergence of inductive loops in Nyquist plots. For the P-PEO coated specimens, the drop in resistance value R_2 was also accelerated in 0.5 M and 1 M NaCl in the early stages of immersion itself viz., within the first 2 h, while the deterioration of resistance R_1 was comparable to those in lower chloride ion concentration solutions (Fig. 12a and 12b). Localized corrosion of the P-PEO coated specimen was found to be induced at 5 h of immersion both in 0.5 M and 1 M NaCl solutions (Fig. 5b). As is seen in the cross-sectional microstructure and the schematic representation, the inner region of the P-PEO coating was thicker and had numerous defects. The thick and defective inner layer in the P-PEO coating probably had spread extensively the permeated electrolyte at the coating/substrate interface, facilitating hydration of MgO leading the formation of more $Mg(OH)_2$. This process had apparently retarded, slightly, the initiation of localized corrosion in 1 M NaCl solution. After localized corrosion initiated, the resistance R_2 decreased continuously with immersion time to very low values in 0.5 M and 1 M NaCl solutions. It has to be highlighted that the resistance R_1 in 1 M NaCl solution was higher and that the R_1 in 0.5 M NaCl solution was close to that in 1 M NaCl solution at the end of 50 h of immersion/EIS testing. It is believed that the formation of more corrosion products in the localized corrosion sites possibly had retarded the permeation process of corrosive electrolyte to the substrate, providing higher resistance of corrosion products layer (R_1) **[35,36]**, which is schematically depicted in Fig. 12b.

4. Conclusions

The current investigation as a whole clearly showed that the corrosion deterioration of the DC pulse PEO coated magnesium alloy in NaCl solution was significantly influenced by chloride ion concentration of the corrosive electrolyte and was also strongly dependent on the characteristics (microstructural and phase composition) of PEO coatings. In lower chloride ion concentration solutions (0.01 M and 0.1 M NaCl), because the corrosive electrolytes are too mild to break down the PEO coatings, the corrosion deterioration of PEO coated specimens was dictated by the degradation of PEO coatings, especially in inner regions of the coating. Therefore, due to the denser and more compact inner layer in the Si-PEO coating combined with the better chemical stability of the composition, the corrosion resistance of the Si-PEO coating was superior and the corrosion deterioration was slower than that of the P-PEO coating in mild corrosive electrolytes. In the more concentrated electrolytes (0.5 M and 1 M NaCl), however, the permeation of higher concentration of chloride ions into the coating/substrate interface

induced the quick breakdown of PEO coatings and caused a localized damage on the underneath magnesium alloy substrate. With the initiation of localized corrosion, high stresses were developed as a consequence of formation of corrosion products at the coating/substrate interface and lifted/damaged the PEO coating, thus exposing the Mg alloy substrate to undergo further deterioration. Based on this investigation, it is concluded that the Si-PEO and P-PEO coatings cannot provide a long-term protection to the magnesium alloy substrate in neutral environments containing high chloride concentrations.

Acknowledgements

J. Liang and P. Bala Srinivasan express their sincere thanks to the Hermann-von-Helmholtz Association, Germany and DAAD, Germany for the award of fellowship and funding. The technical support of Mr. V. Heitmann and Mr. U. Burmester during the course of this work is gratefully acknowledged.

References

[1] D. Eliezer, E. Aghion, F.H. Froes, Adv. Perform. Mater. 5 (1998) 201.

[2] B.L. Mordike, T. Ebert, Maqster. Sci. Eng. A 302 (2001) 37.

[3] G. Song, A. Atrens, Adv. Eng. Mater. 1 (1999) 11.

[4] G. Song, A. Atrens, Adv. Eng. Mater. 5 (2003) 837.

[5] R. Ambat, N.N. Aung, W. Zhou, J. Appl. Electrochem. 30 (2000) 865.

[6] G. Song, A. Atrens, D. StJohn, J. Nairn, Y. Lang, Corros. Sci. 39 (1997) 855.

[7] G. Song, A. Atrens, D. StJohn, X. Wu, J. Nairn, Corros. Sci. 39 (1997) 1981.

[8] G. Baril, N. Pebere, Corros. Sci. 43 (2001) 471.

[9] H. Altun, S. Sen, Mater. Design 25 (2004) 637.

[10] G. Song, D. StJohn, Corros. Sci. 46 (2004) 1381.

[11] M. Zhao, M. Liu , G. Song, A. Atrens, Corros. Sci. 50 (2008) 3168.

[12] J. Chen, J.Q. Wang, E.H. Han, J.H. Dong, W. Ke, Electrochim. Acta 52 (2007) 3299.

[13] J.E. Gray, B. Luan, J. Alloys Compd. 336 (2002) 88.

[14] G. Song, Corrosion and Protection of Magnesium Alloys, Chemical Industry Press, Beijing, 2006. pp. 237-254 (in Chinese).

[15] A.L. Yerokhin, X. Nie, A. Leyland, A. Matthews, S. J. Dowey, Surf. Coat. Technol. 122 (1999) 73.

[16] C. Blawert, W. Dietzel, E. Ghali, G. Song, Adv. Eng. Mater. 8 (2006) 511.

[17] P. Gupta, G. Tenhundfeld, E.O. Daigle, D. Ryabkov, Surf. Coat. Technol. 201 (2007) 8746.

[18] A. Kuhn, Met. Finish. 101 (2003) 44.

[19] J. Liang, L. Hu, J. Hao, Appl. Surf. Sci. 253 (2007) 4490.

[20] Q.Z. Cai, L.S. Wang, B.K. Wei, Q.X. Liu, Surf. Coat. Technol. 200 (2006) 3727.

[21] J. Liang, P. Bala Srinivasan, C. Blawert, W. Dietzel, Electrochim. Acta 54 (2009) 3842.

[22] J. Liang, B.G. Guo, J. Tian, H.W. Liu, J.F. Zhou, W.M. Liu, T. Xu, Surf. Coat. Technol. 199 (2005) 121.

[23] H.P. Duan, K.Q. Du, C.W. Yan, F.H. Wang, Electrochim. Acta 51 (2006) 2898.

[24] F.A. Bonilla, A. Berkani, Y. Liu, P. Skeldon, G.E. Thompson, H. Habazaki, K. Shimizu, C. John, K. Stevens, J. Electrochem. Soc. 149 (2002) B4.

[25] R. Arrabal , E. Matykina, F. Viejo, P. Skeldon, G.E. Thompson, Corros. Sci. 50 (2008) 1744.

[26] E. Ghali, W. Dietzel, K.U. Kainer, J. Mater. Eng. Perform. 13 (2004) 7.

[27] G.-L Song, Surf. Coat. Technol. 203 (2009) 3618.

[28] G.-L Song, Corros. Sci. 51 (2009) 2063.

[29] C.N. Cao, J.Q. Zhang, An Introduction to Electrochemical Impedance Spectroscopy, Science Press, Beijing, 2002. pp. 158 (in Chinese).

[30] G. Baril, C. Blanc, N. Pébère, J. Electrochem. Soc., 148 (2001) B489.

[31] Y.C. Xin, C.L. Liu, W.J. Zhang, K.F. Huo, G.Y. Tang, X.B. Tian, P.K. Chu, J. Mater. Res. 23 (2008) 312.

[32] C.-E. Barchiche, E. Rocca, C. Juers, J. Hazan, J. Steinmetz, Electrochim. Acta 53 (2007) 415.

[33] S.J. Xia, R. Yue, R.G. Rateick, Jr., V.I. Birss, J. Electrochem. Soc. 151 (3) (2004) B179.

[34] J. Liang, P. Bala Srinivasan, C. Blawert, W. Dietzel, Corros. Sci. 51 (2009) 2483.

[35] S.V. Lamaka, G. Knornschild, D.V. Snihirova, M.G. Taryba, M.L. Zheludkevich, M.G. S. Ferreira, Electrochim. Acta 55 (2009) 131.

[36] W.J. Liu, F.H. Cao, L.R. Chang, Z. Zhang, J.Q. Zhang, Corros. Sci. 51 (2009) 1334.

Figure 1a

Click here to download high resolution image

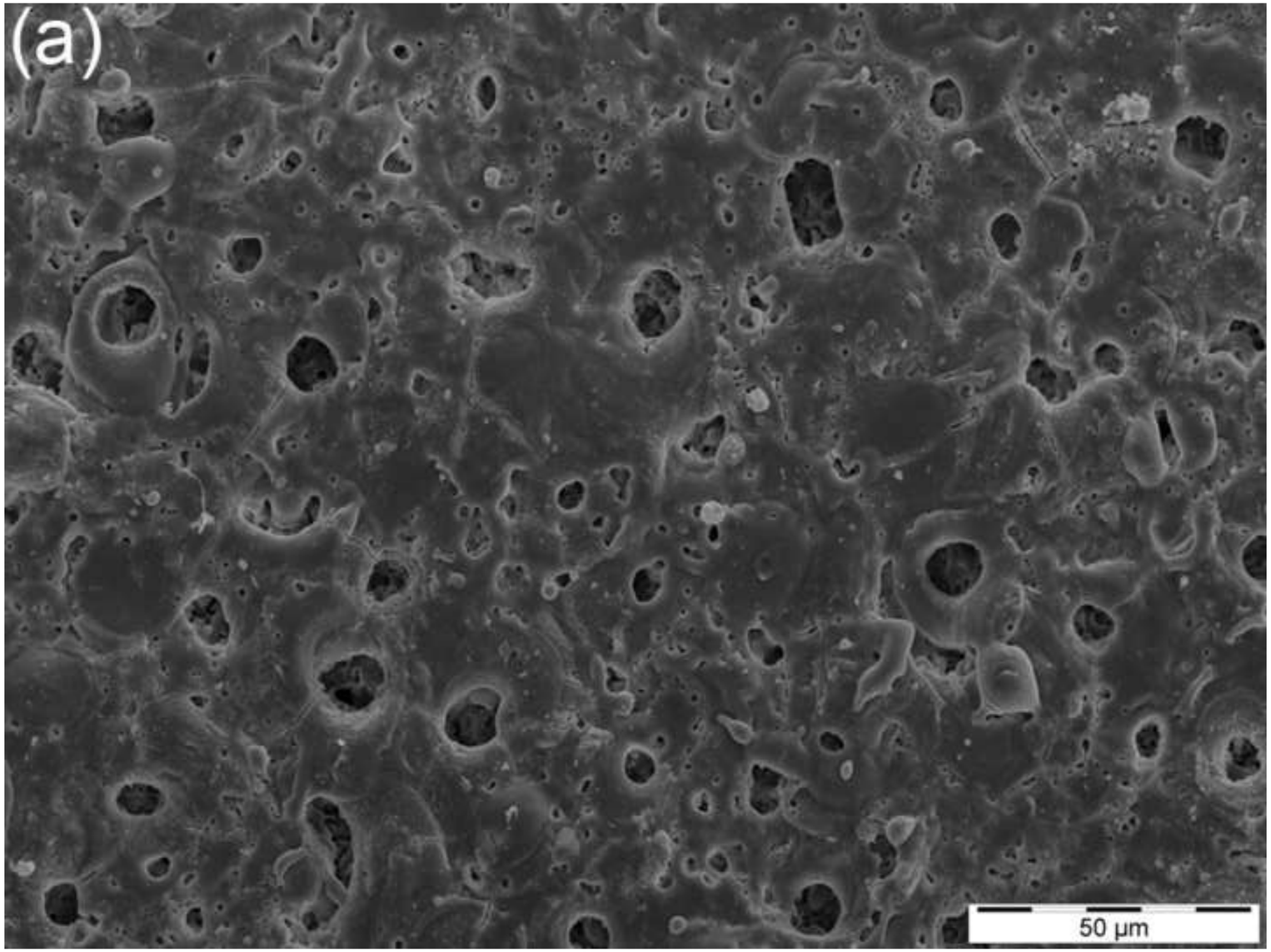

Figure 1b

Click here to download high resolution image

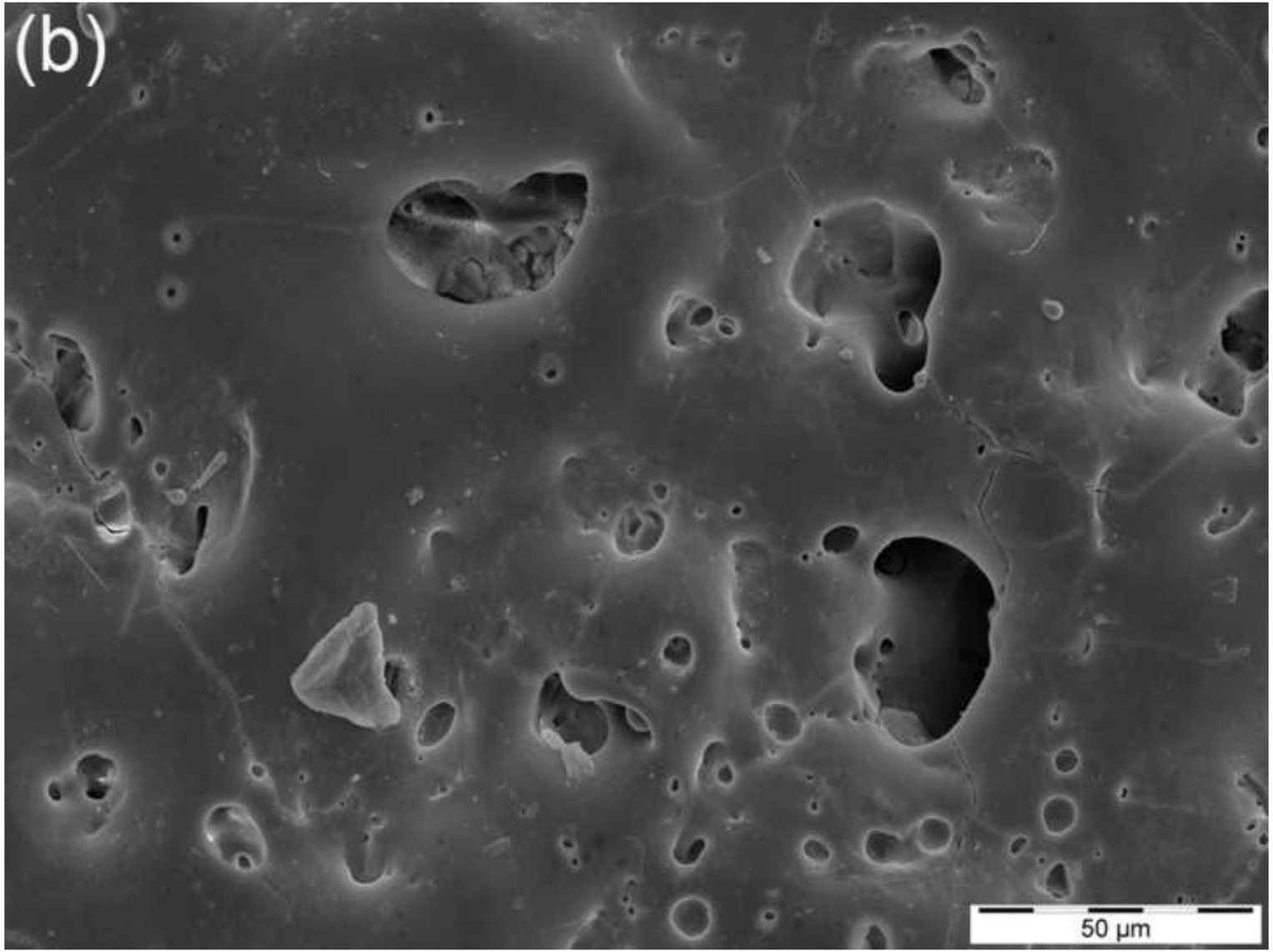

Figure 1c

Click here to download high resolution image

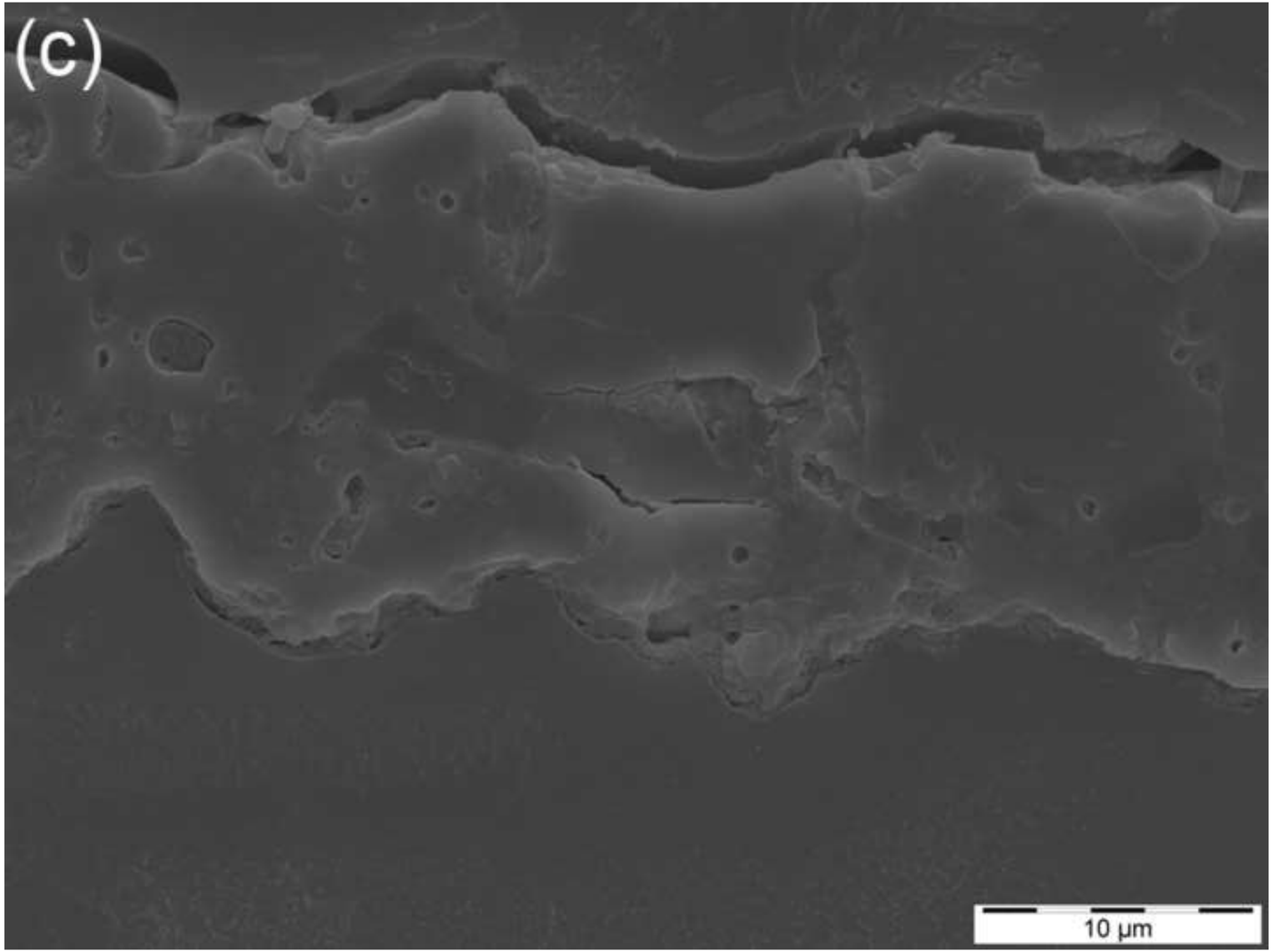

Figure 1d

Click here to download high resolution image

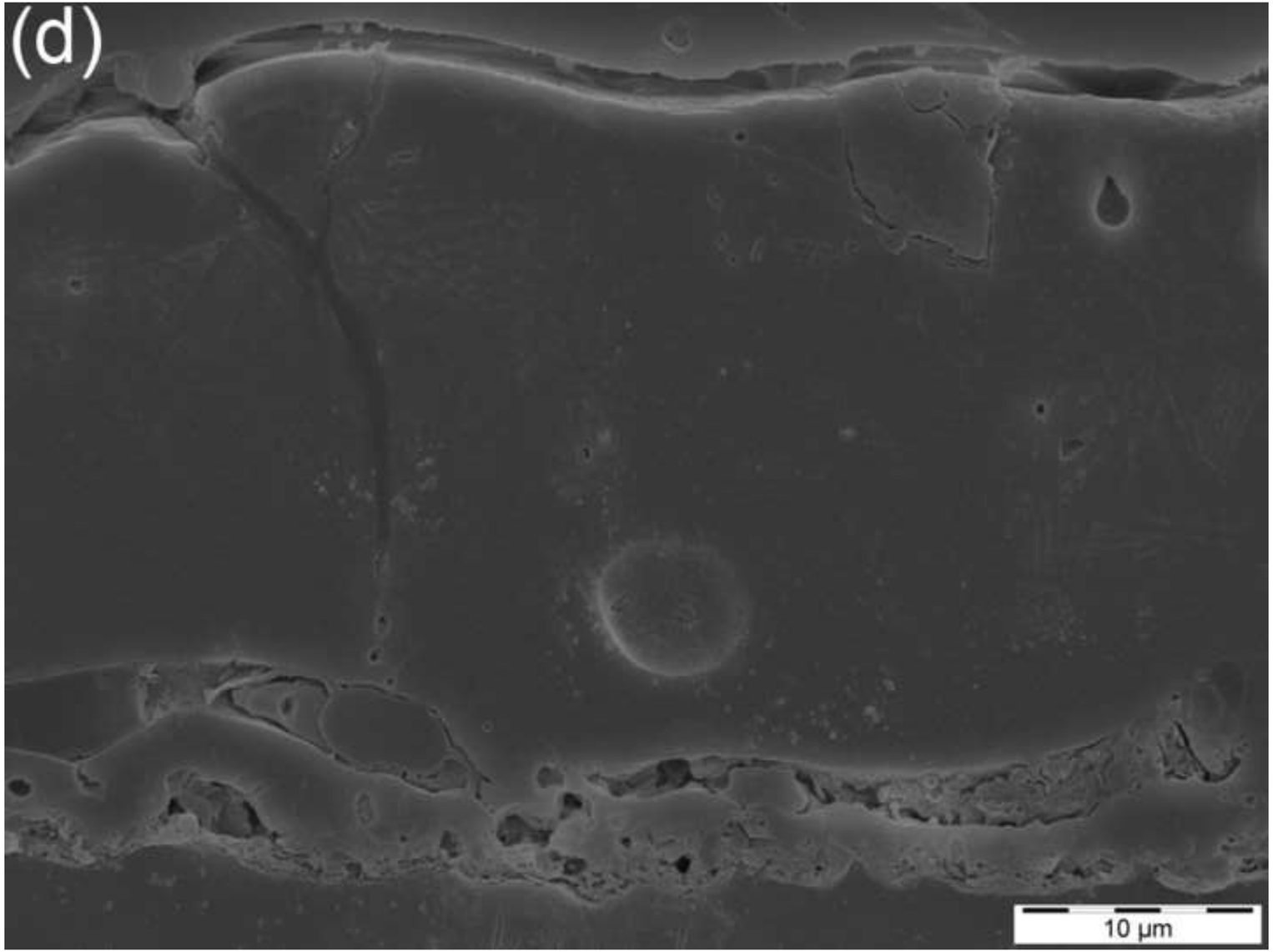

Figure 2a
Click here to download high resolution image

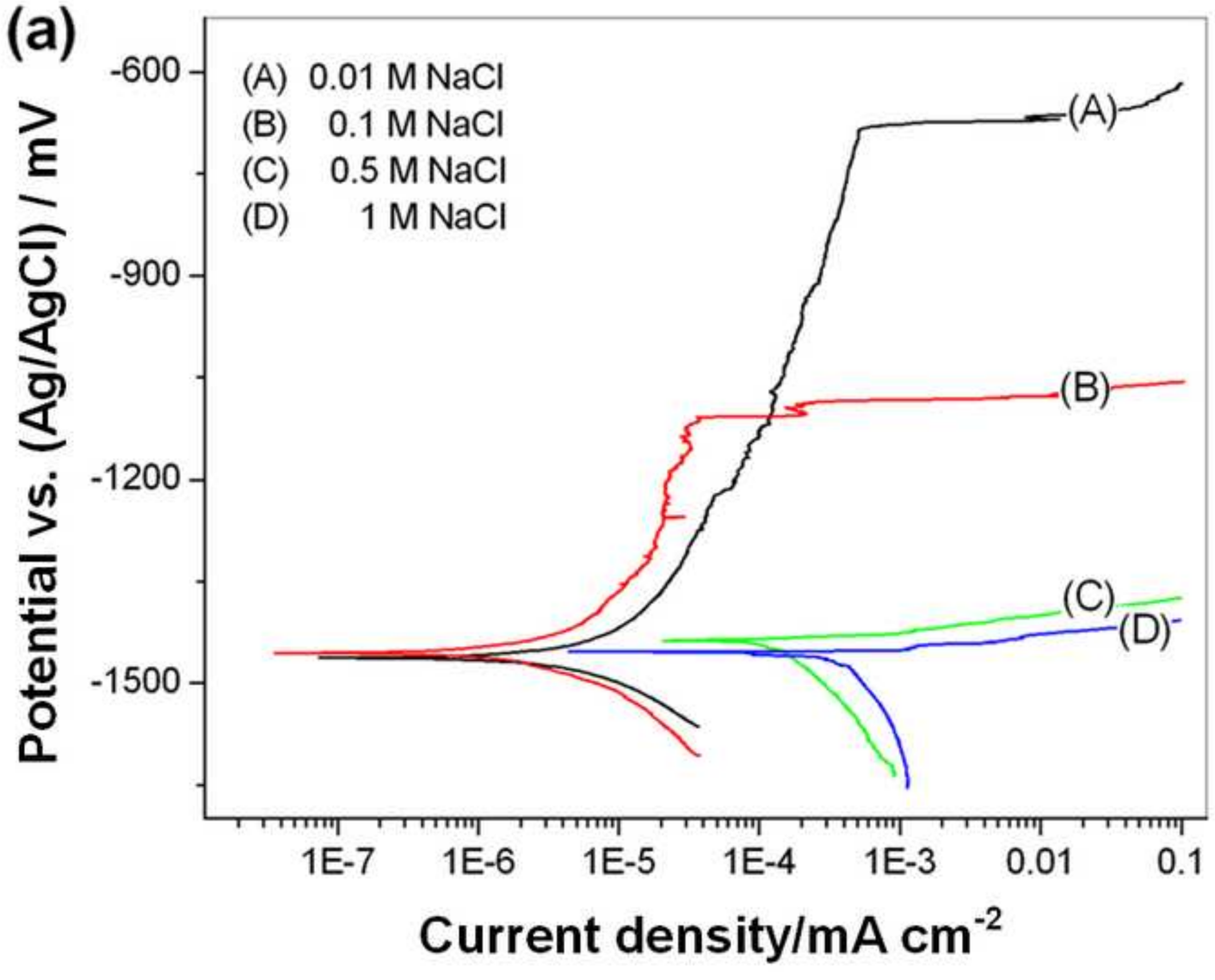

Figure 2b
Click here to download high resolution image

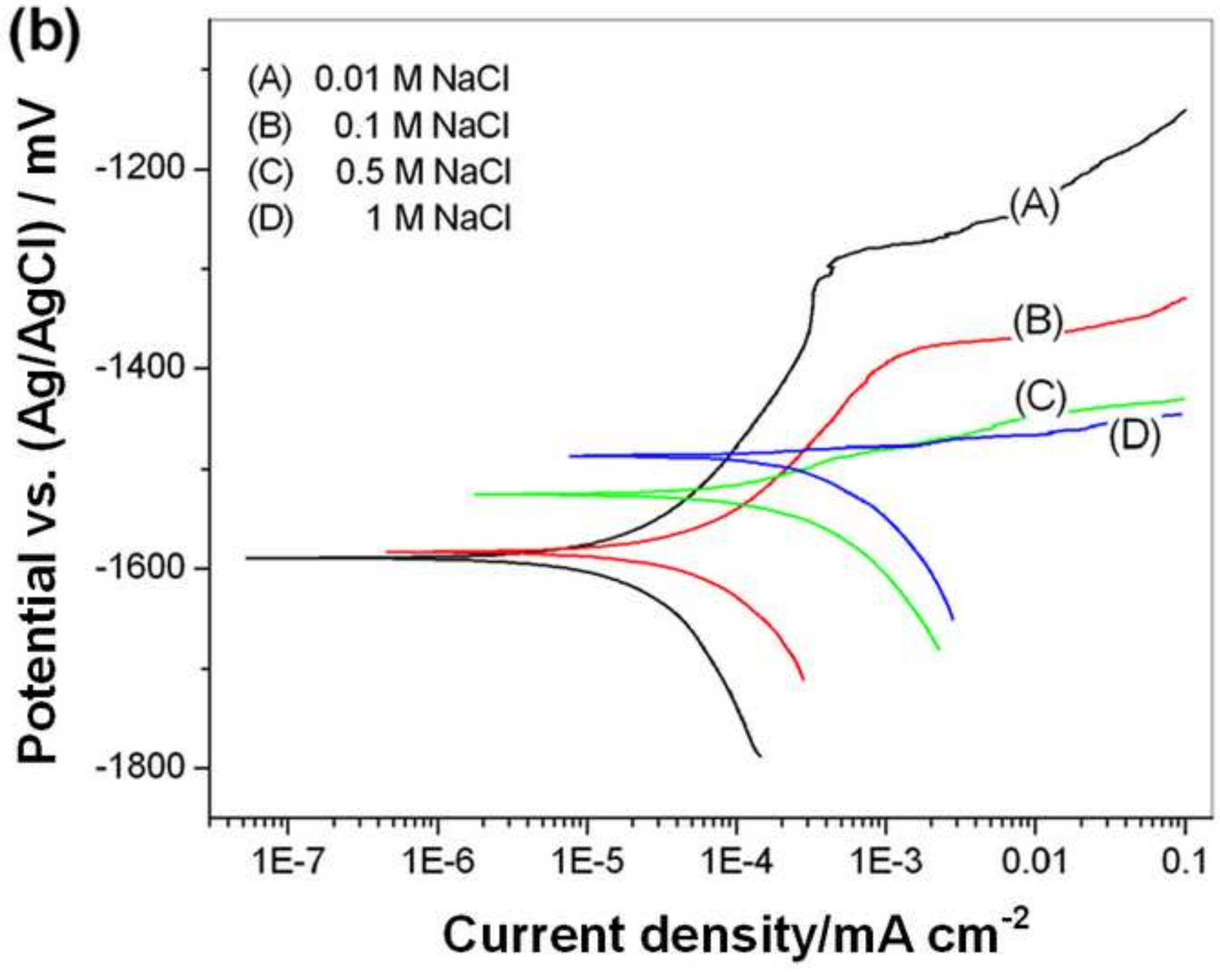

Figure 3a
Click here to download high resolution image

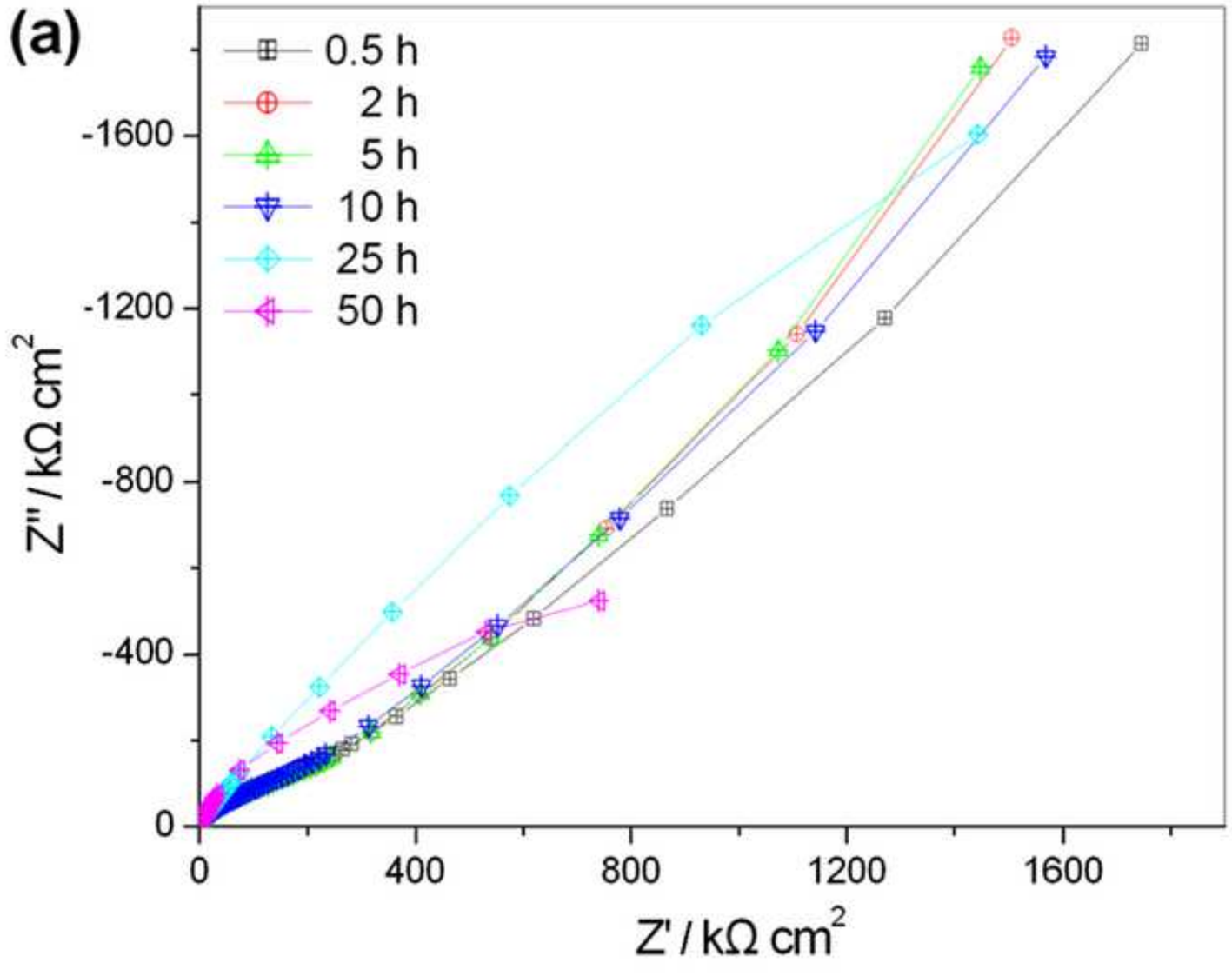

Figure 3b
Click here to download high resolution image

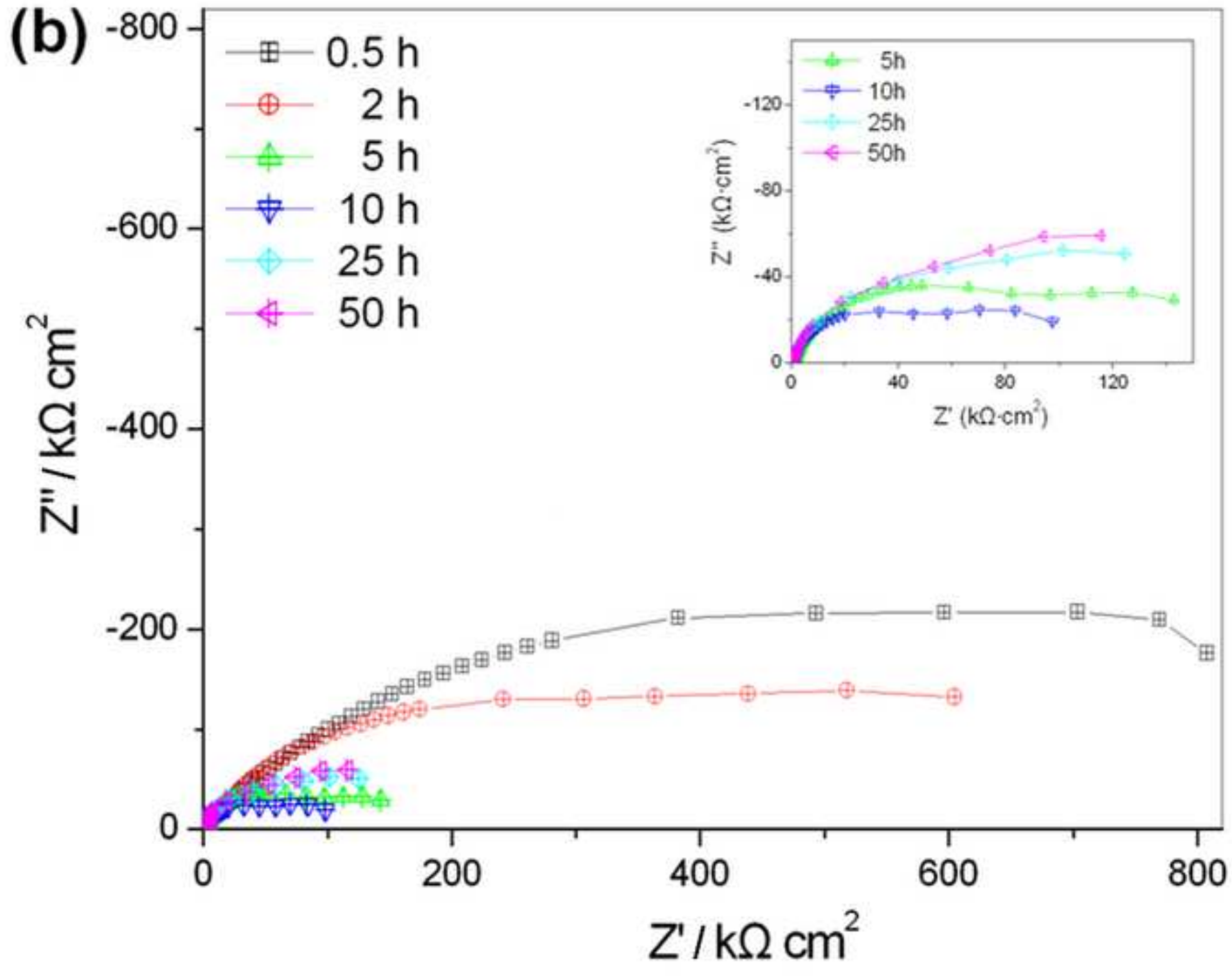

Figure 4a
Click here to download high resolution image

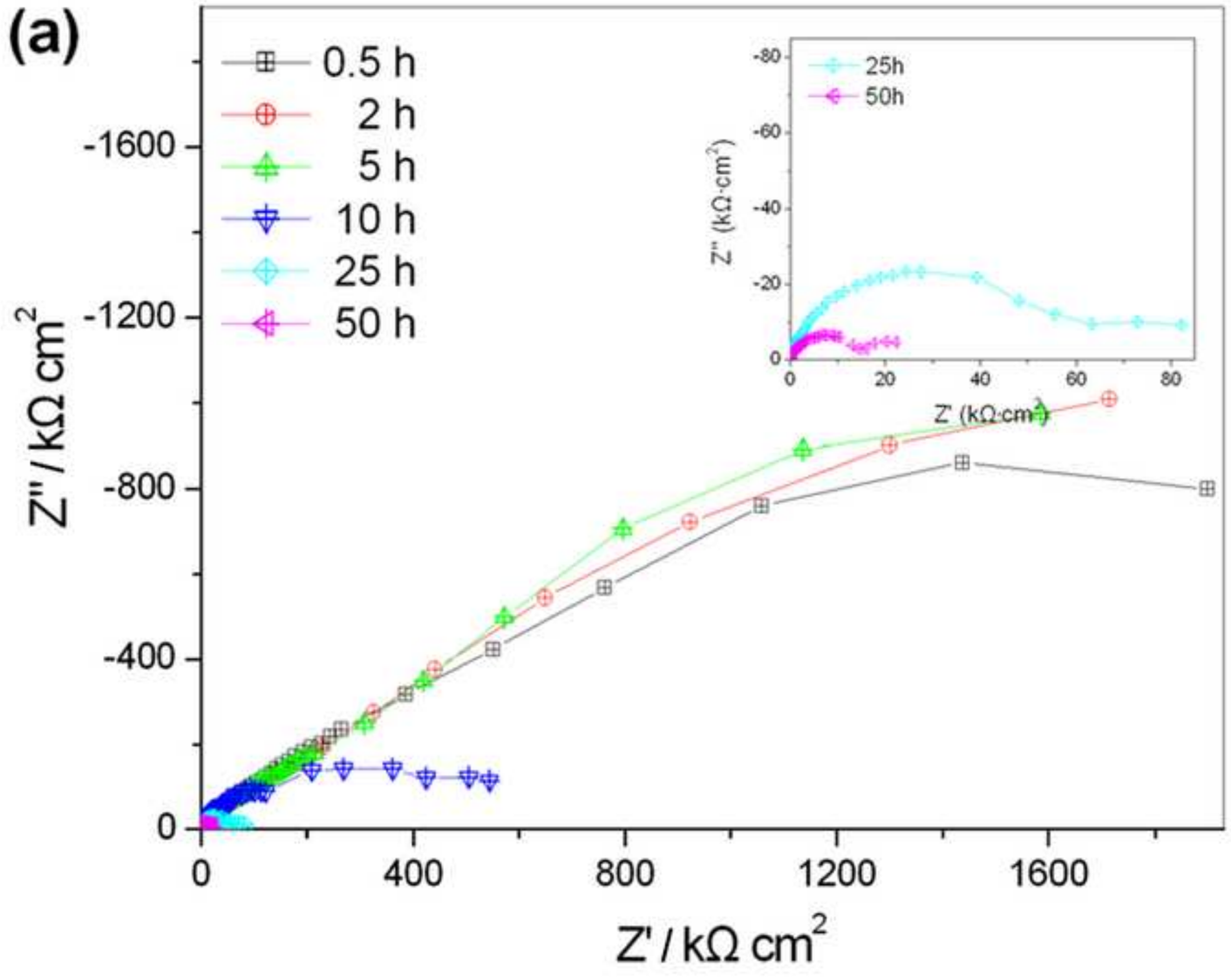

Figure 4b

Click here to download high resolution image

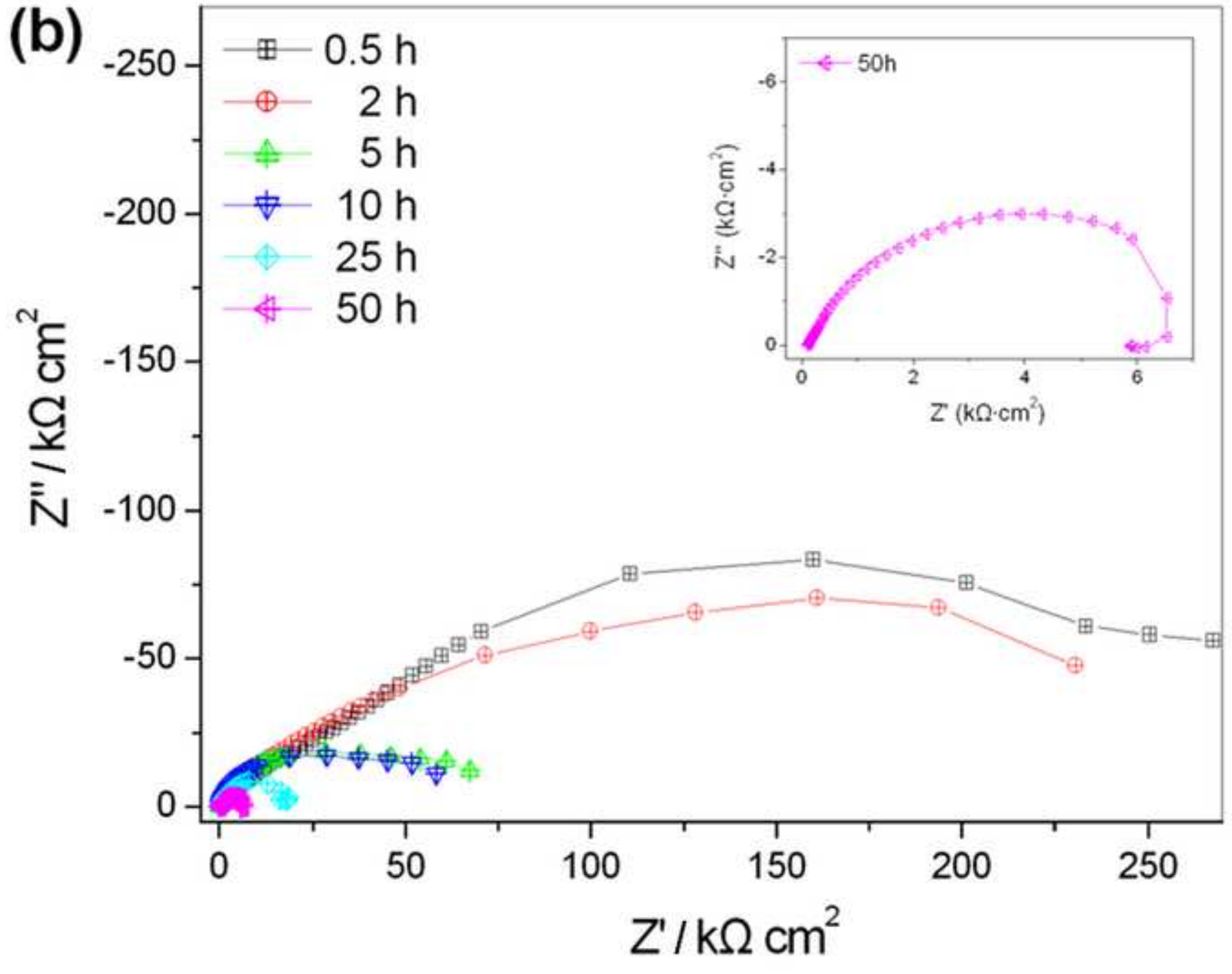

Figure 5a

Click here to download high resolution image

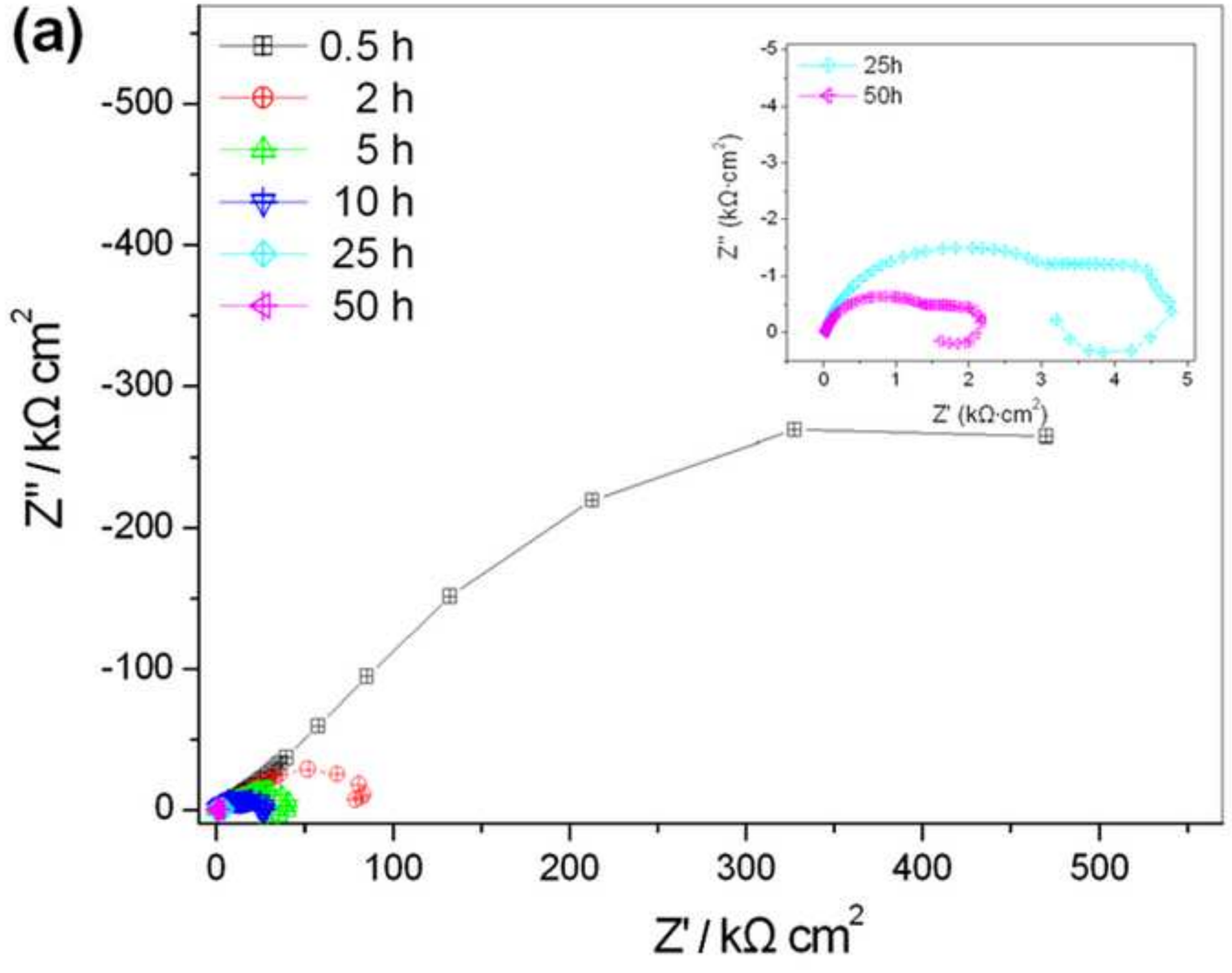

Figure 5b
Click here to download high resolution image

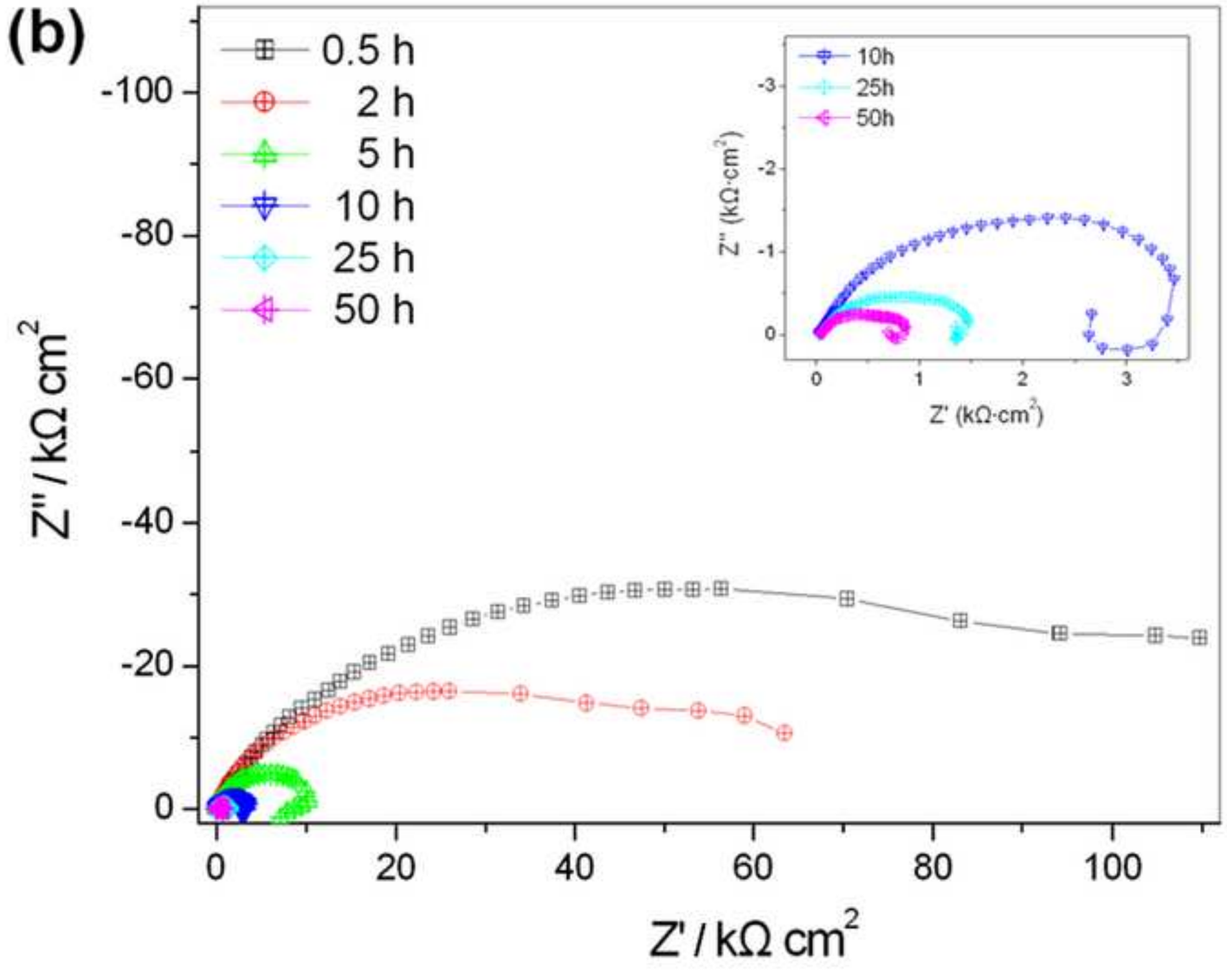

Figure 6a

Click here to download high resolution image

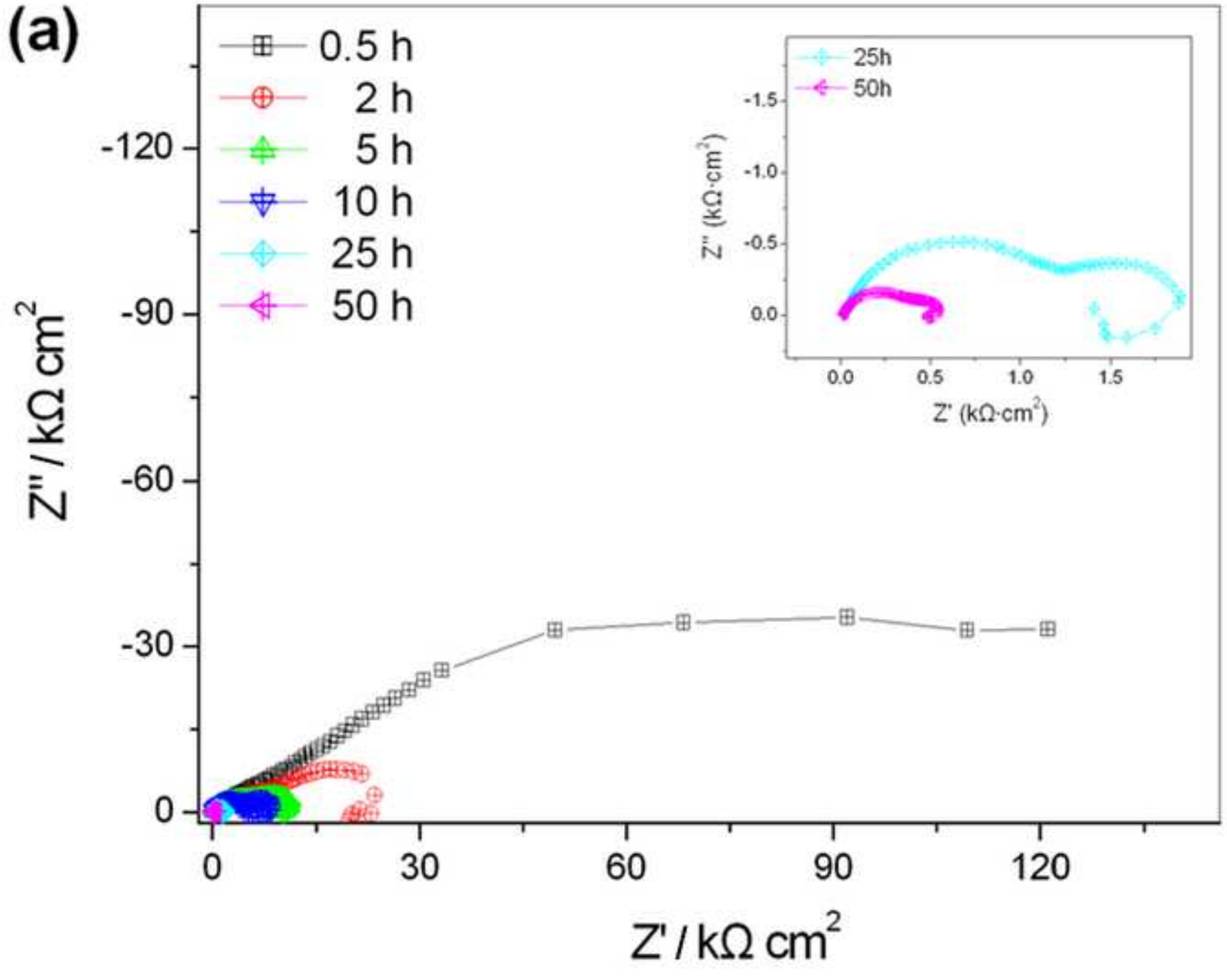

Figure 6b
Click here to download high resolution image

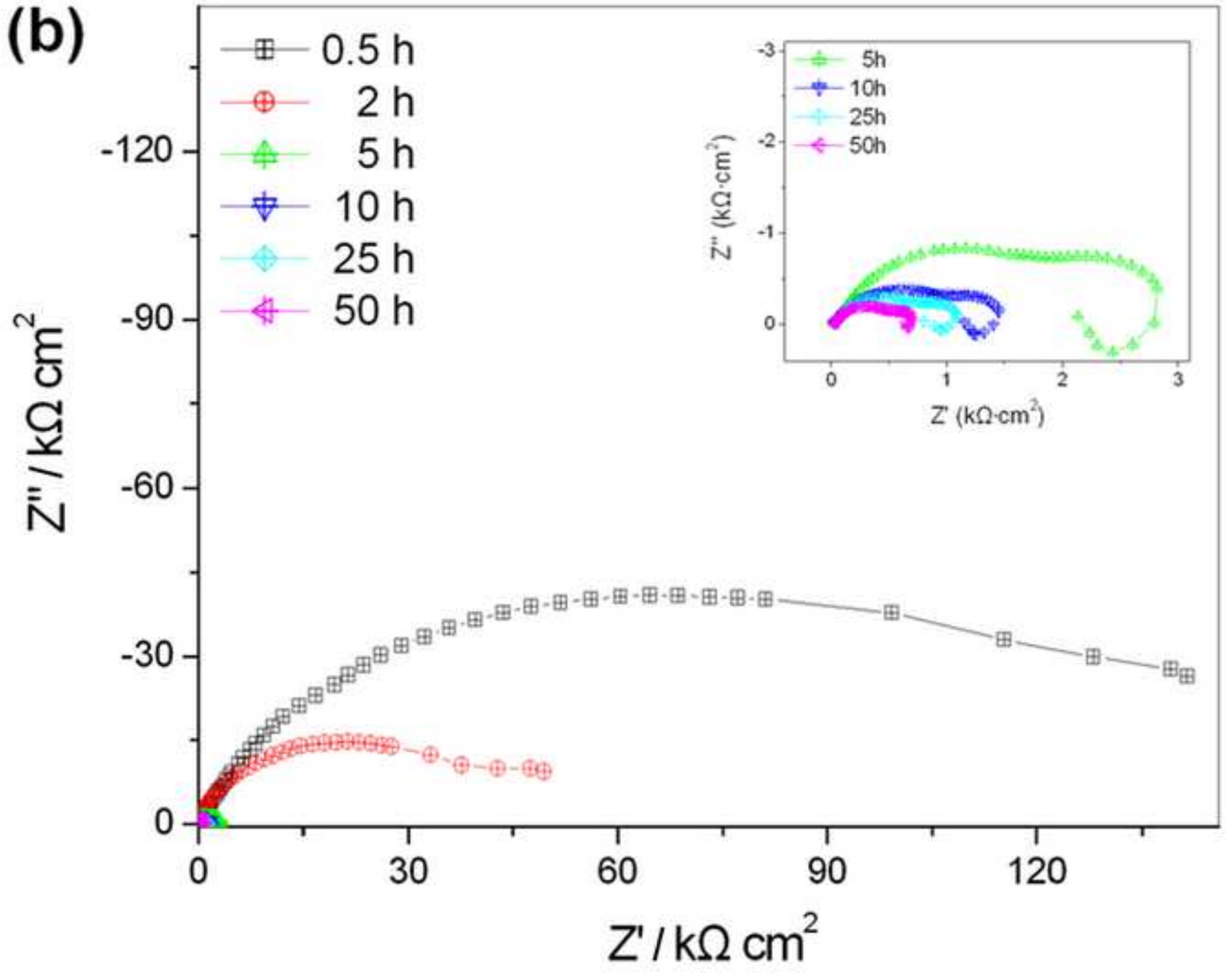

Figure 7
Click here to download high resolution image

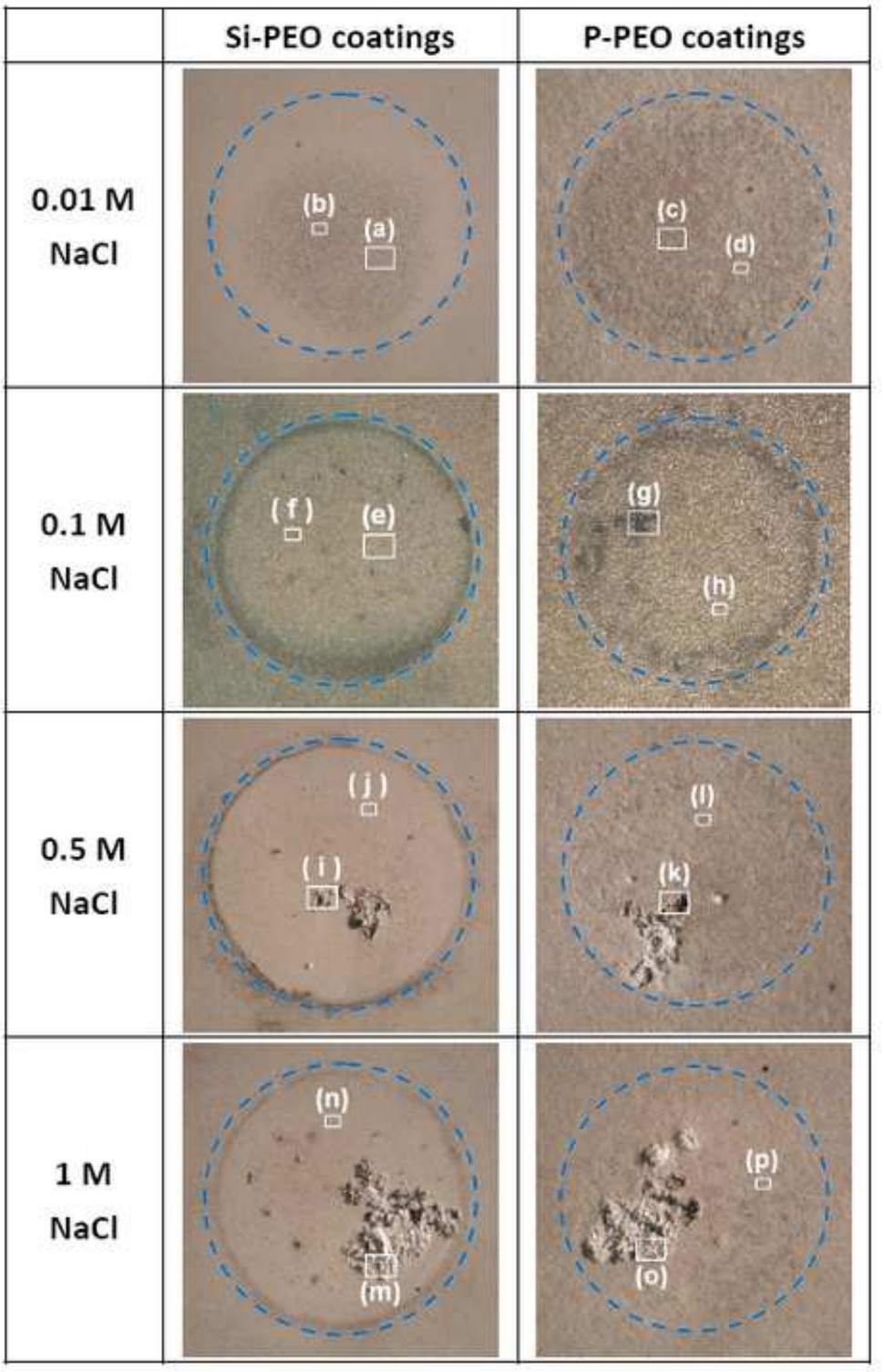

Figure 8

Click here to download high resolution image

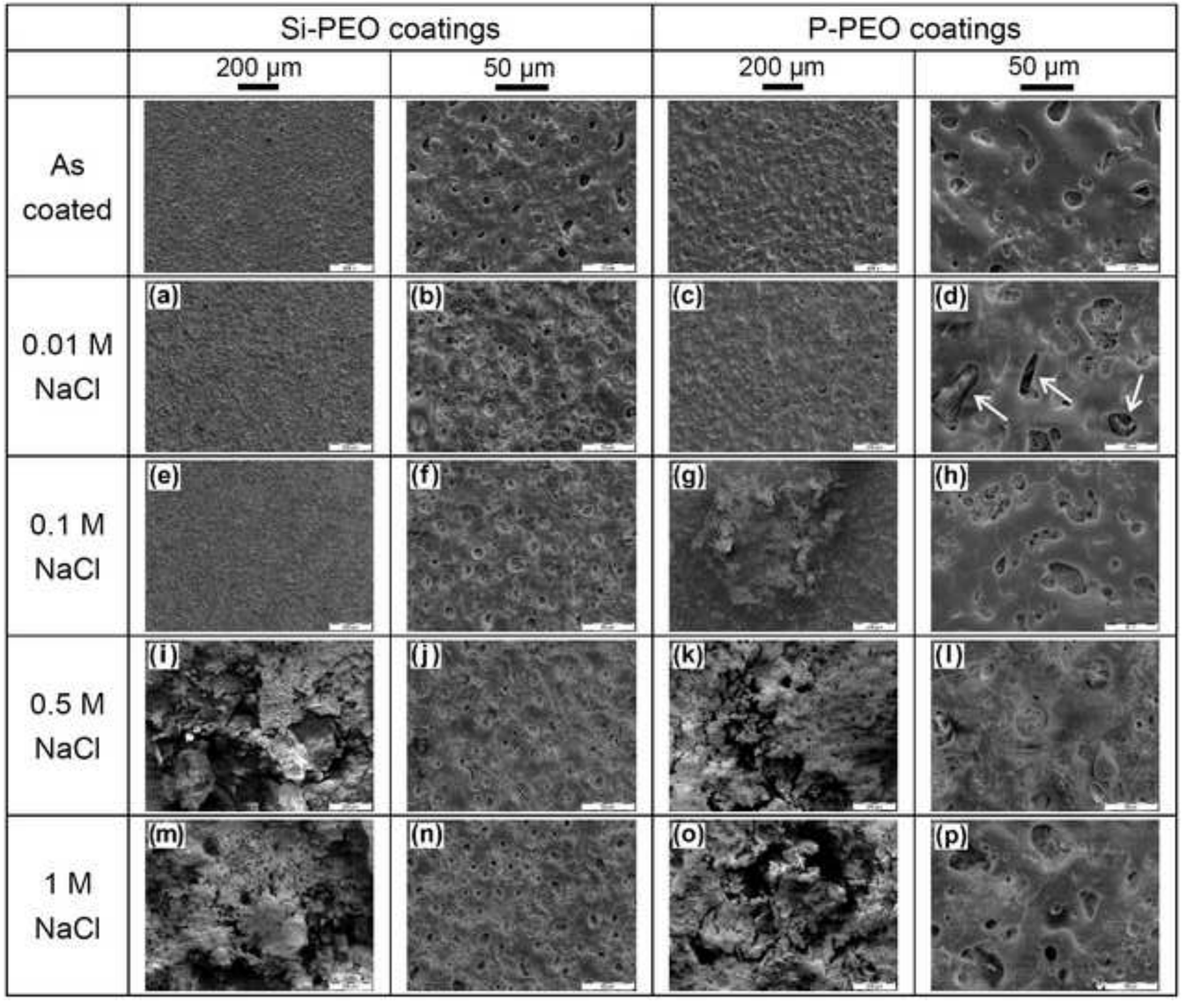

Figure 9a

Click here to download high resolution image

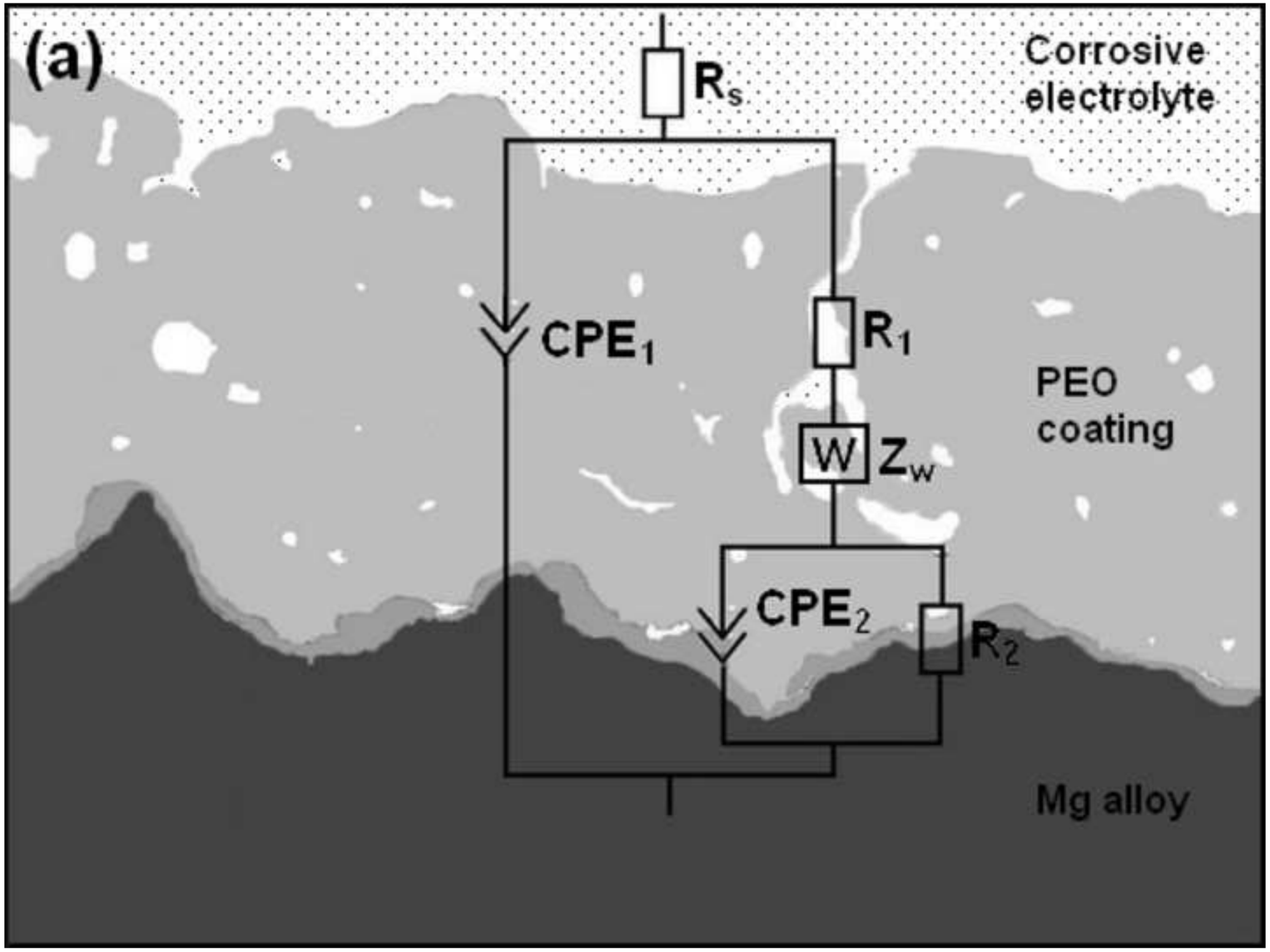

Figure 9b

Click here to download high resolution image

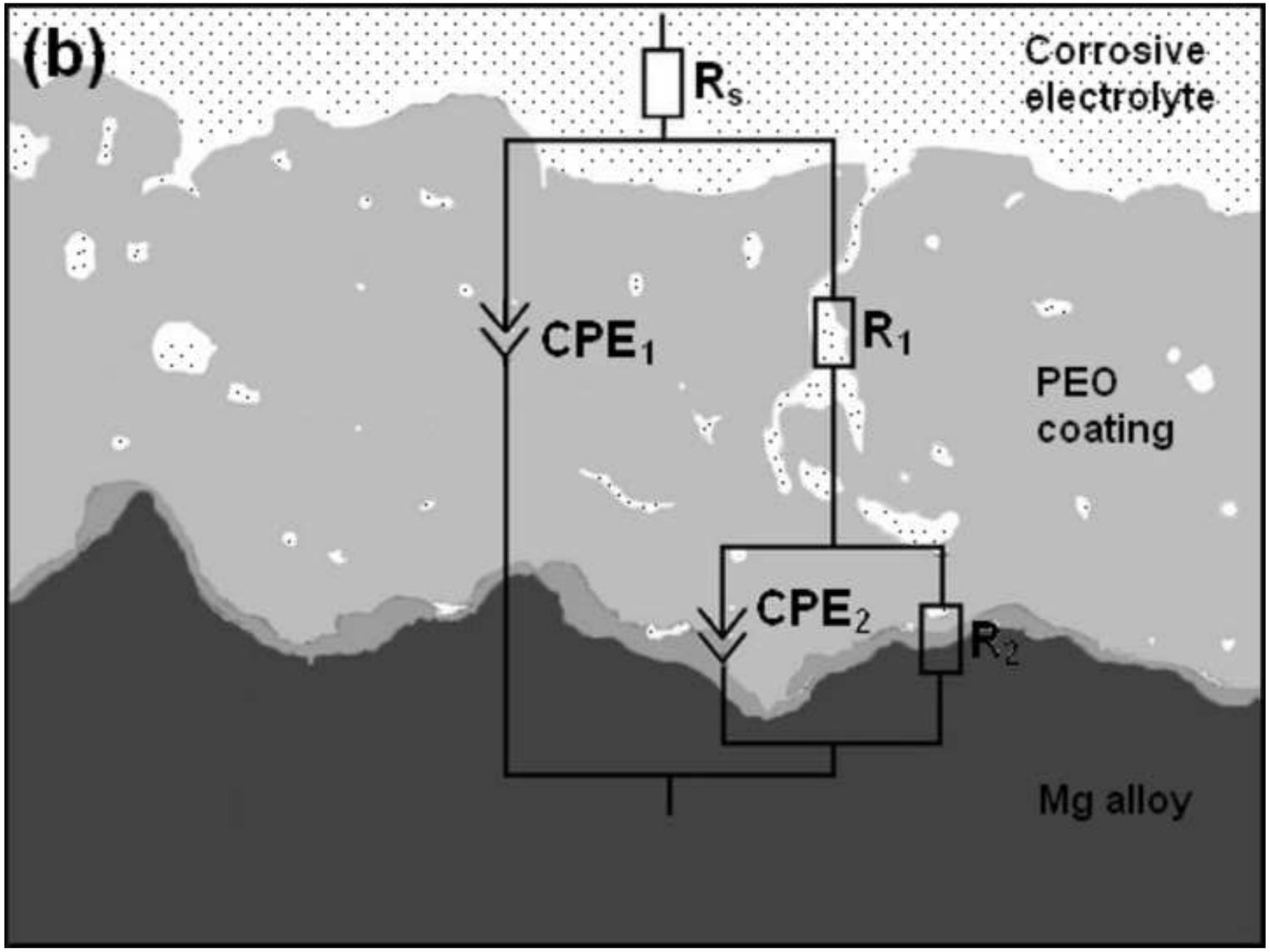

Figure 9c

Click here to download high resolution image

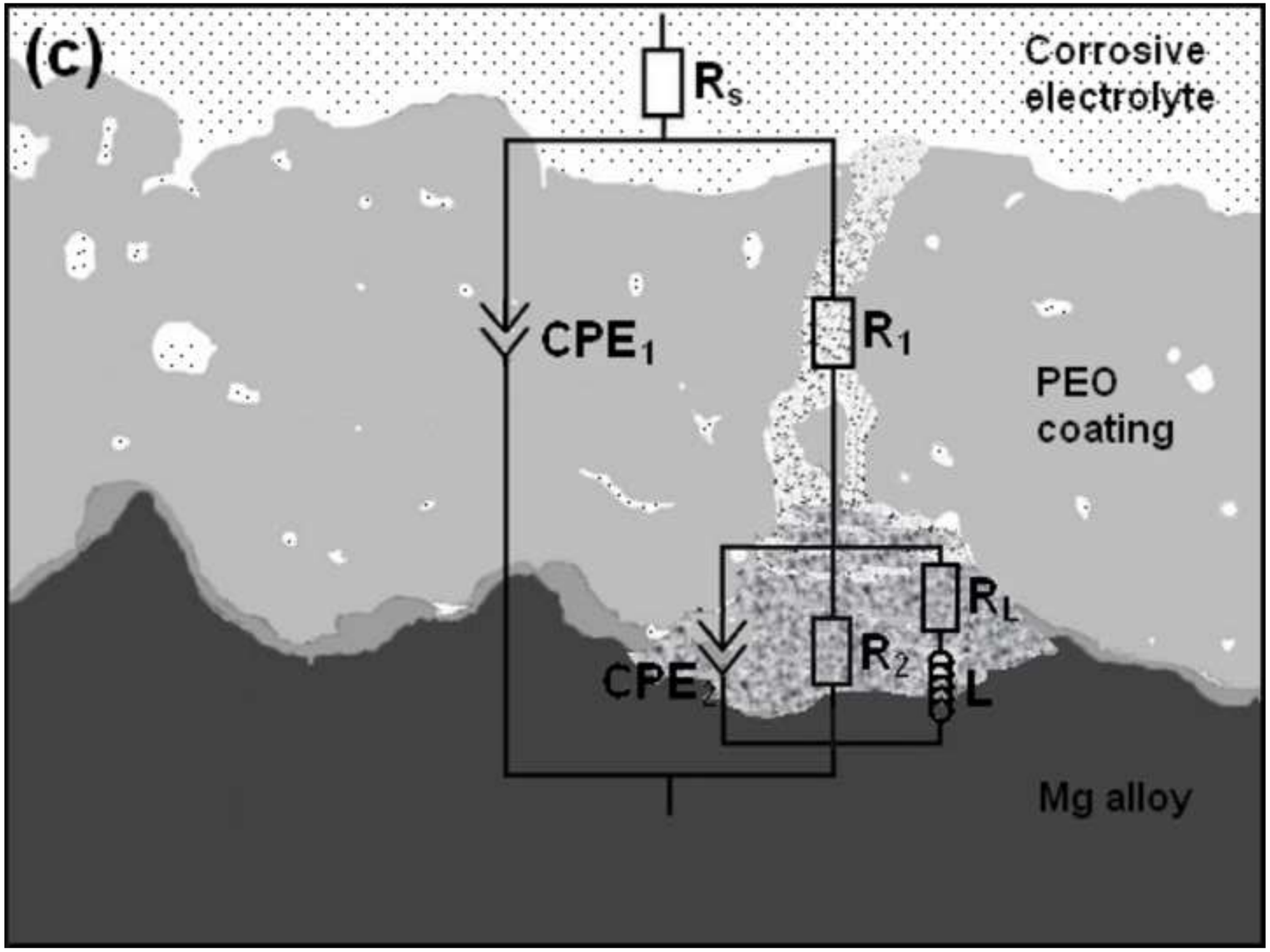

Figure 10a

Click here to download high resolution image

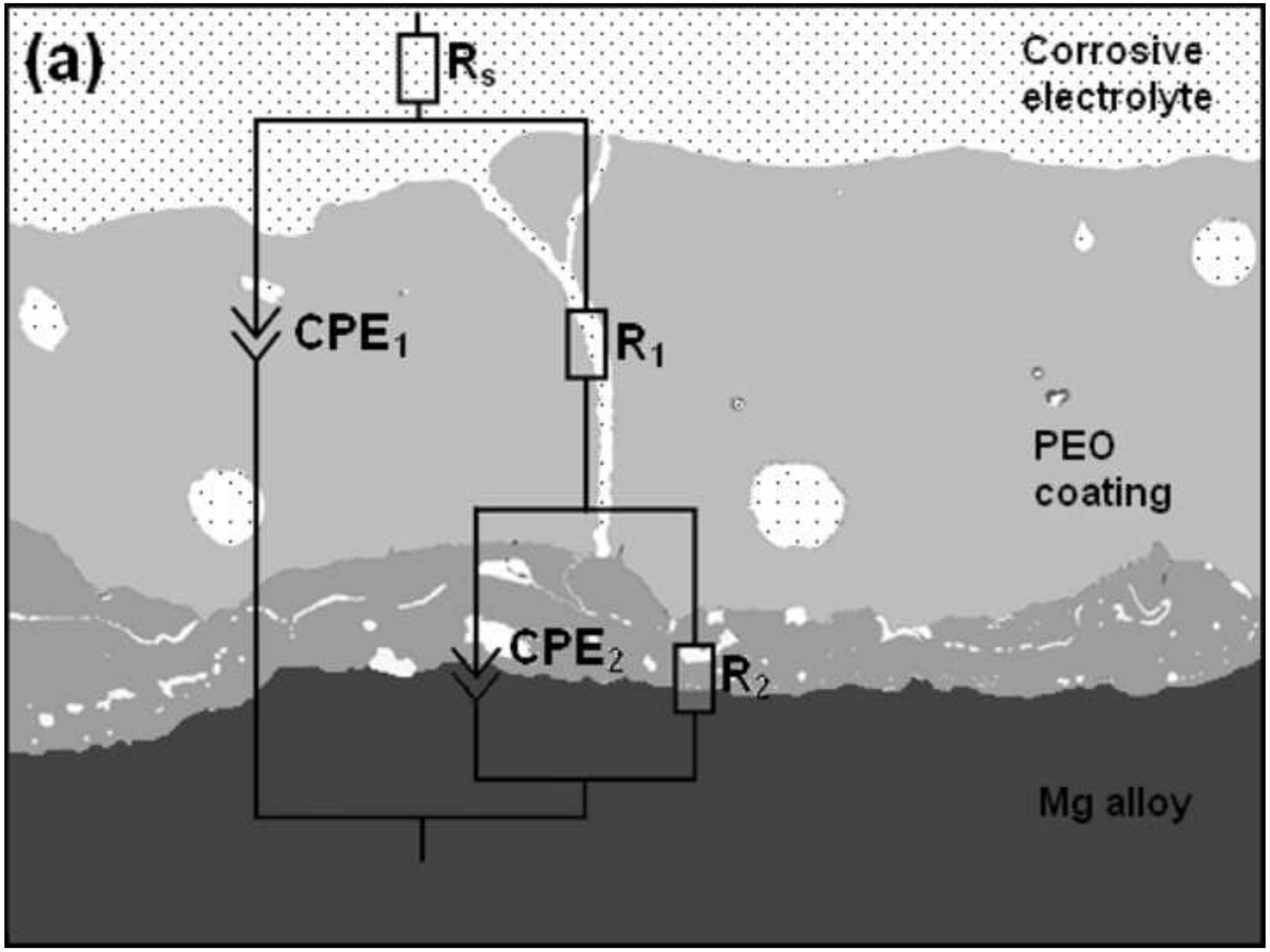

Figure 10b

Click here to download high resolution image

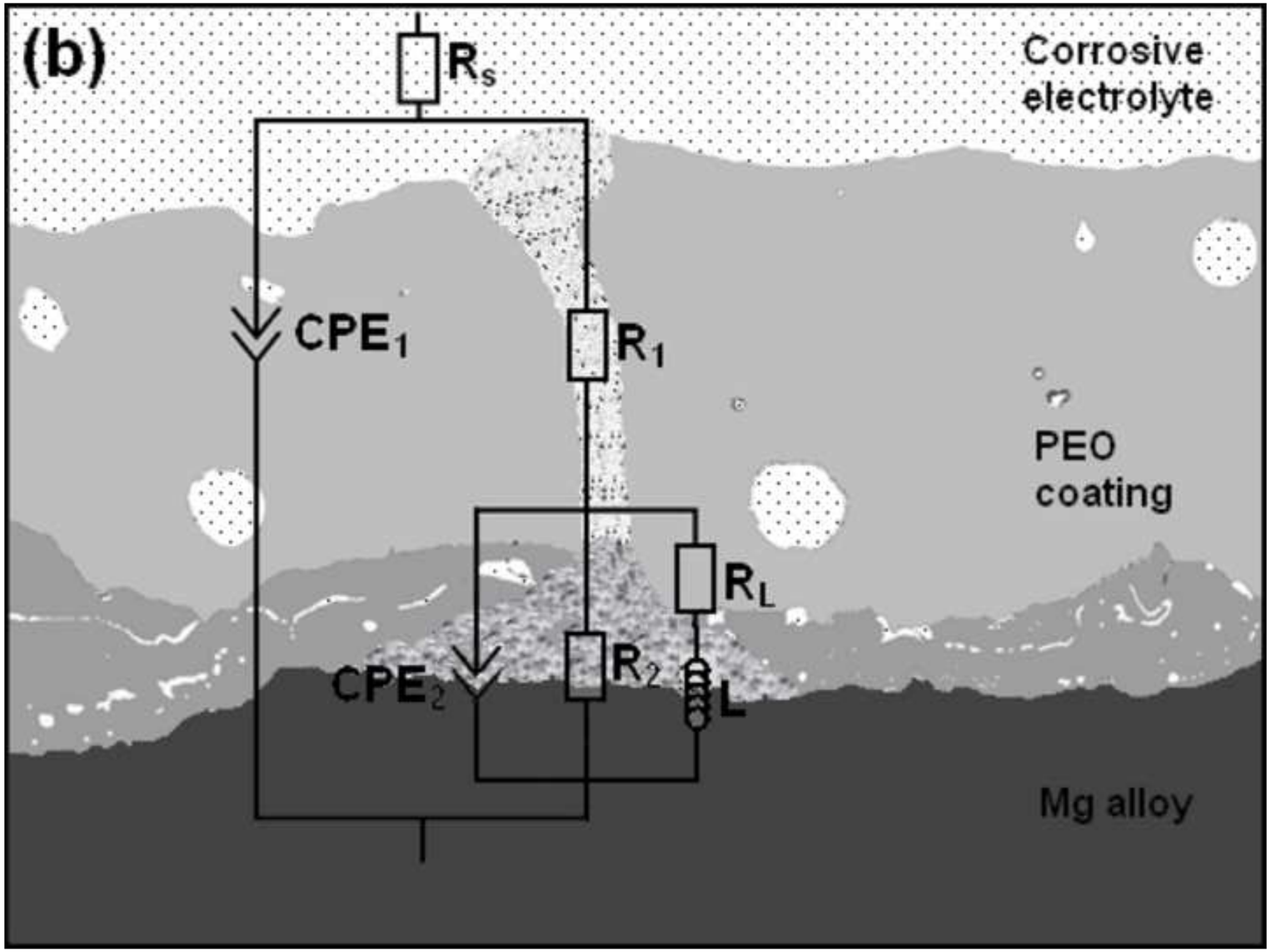

Figure 11a
Click here to download high resolution image

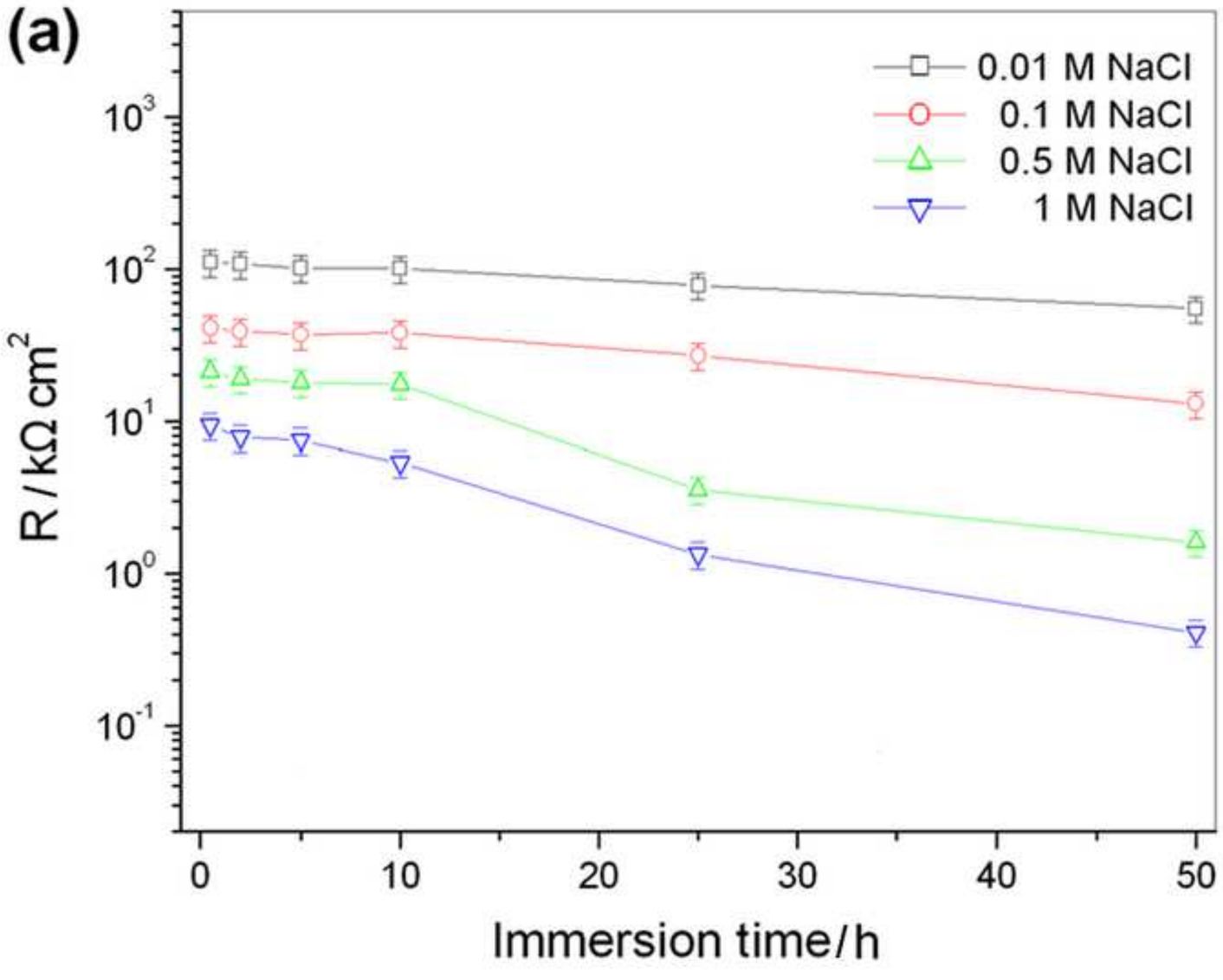

Figure 11b

Click here to download high resolution image

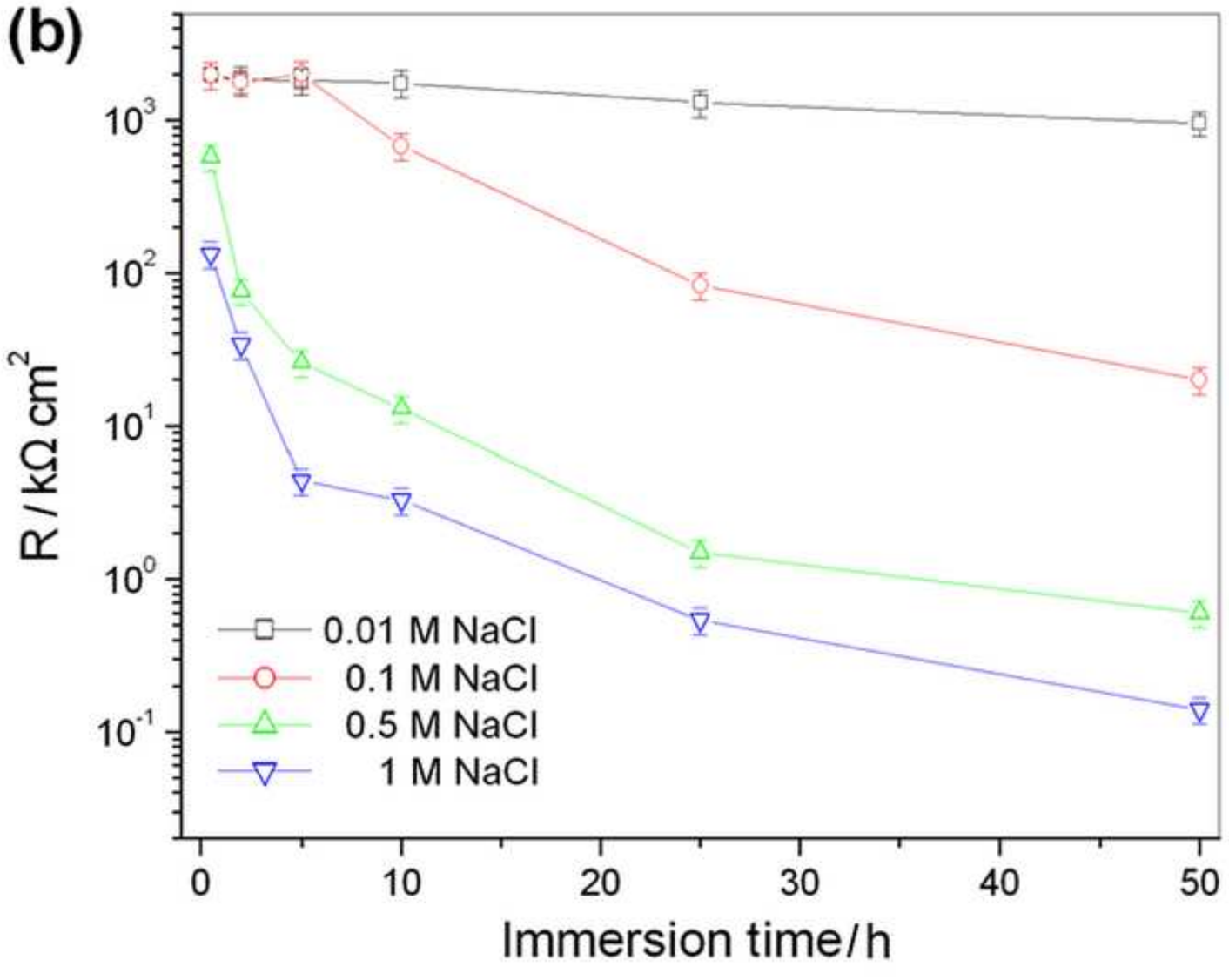

Figure 12a
Click here to download high resolution image

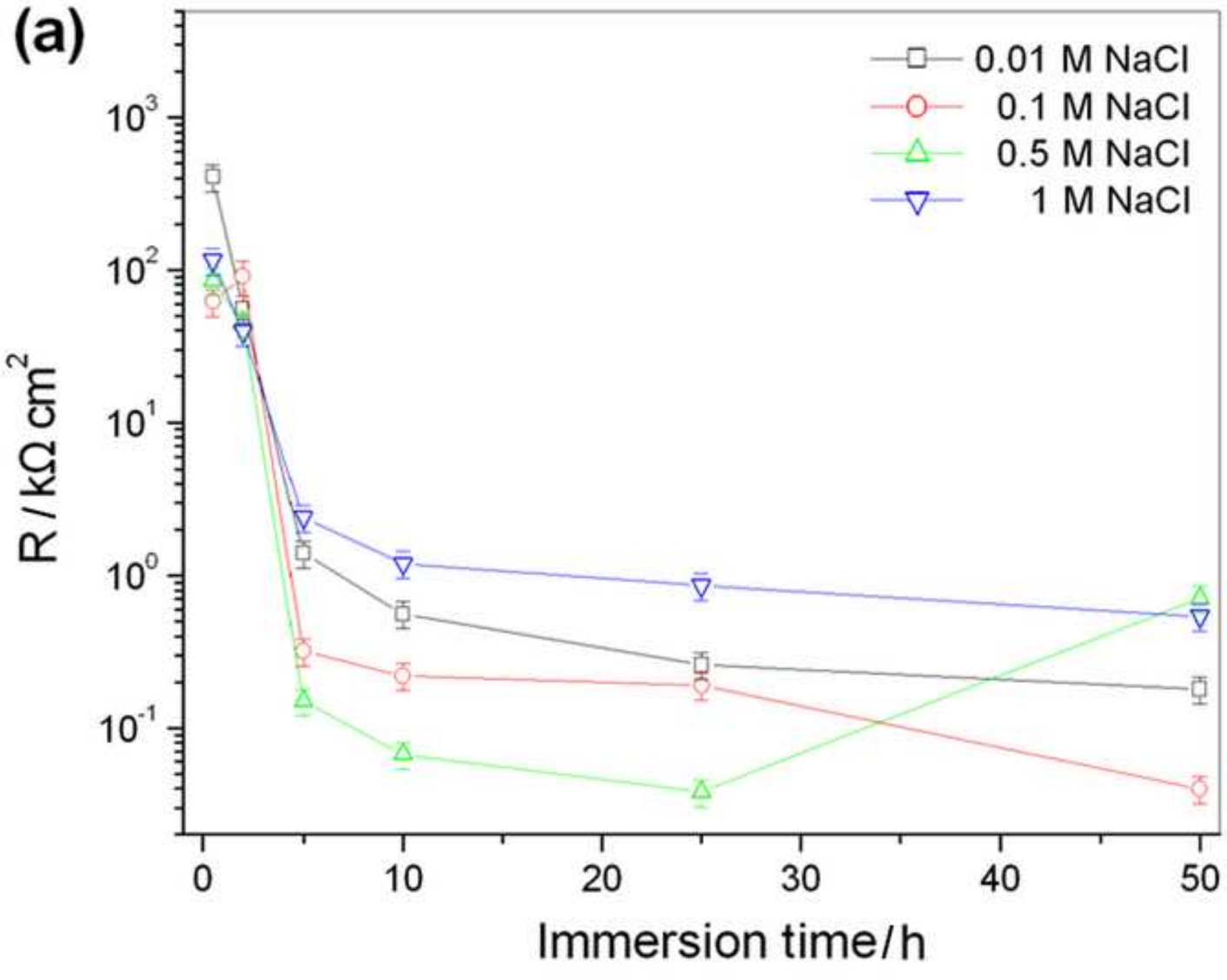

Figure 12b

Click here to download high resolution image

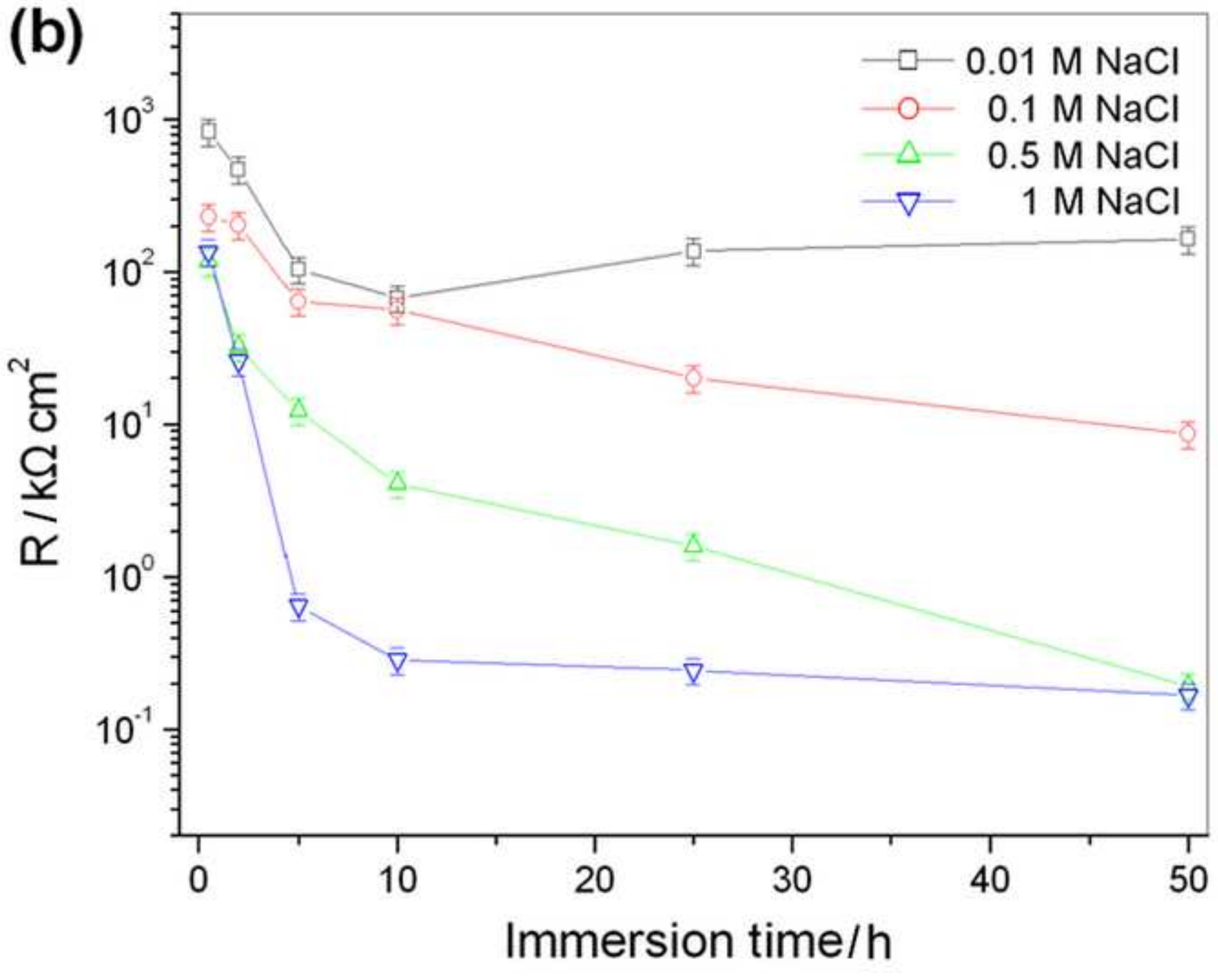

Figure 13a
Click here to download high resolution image

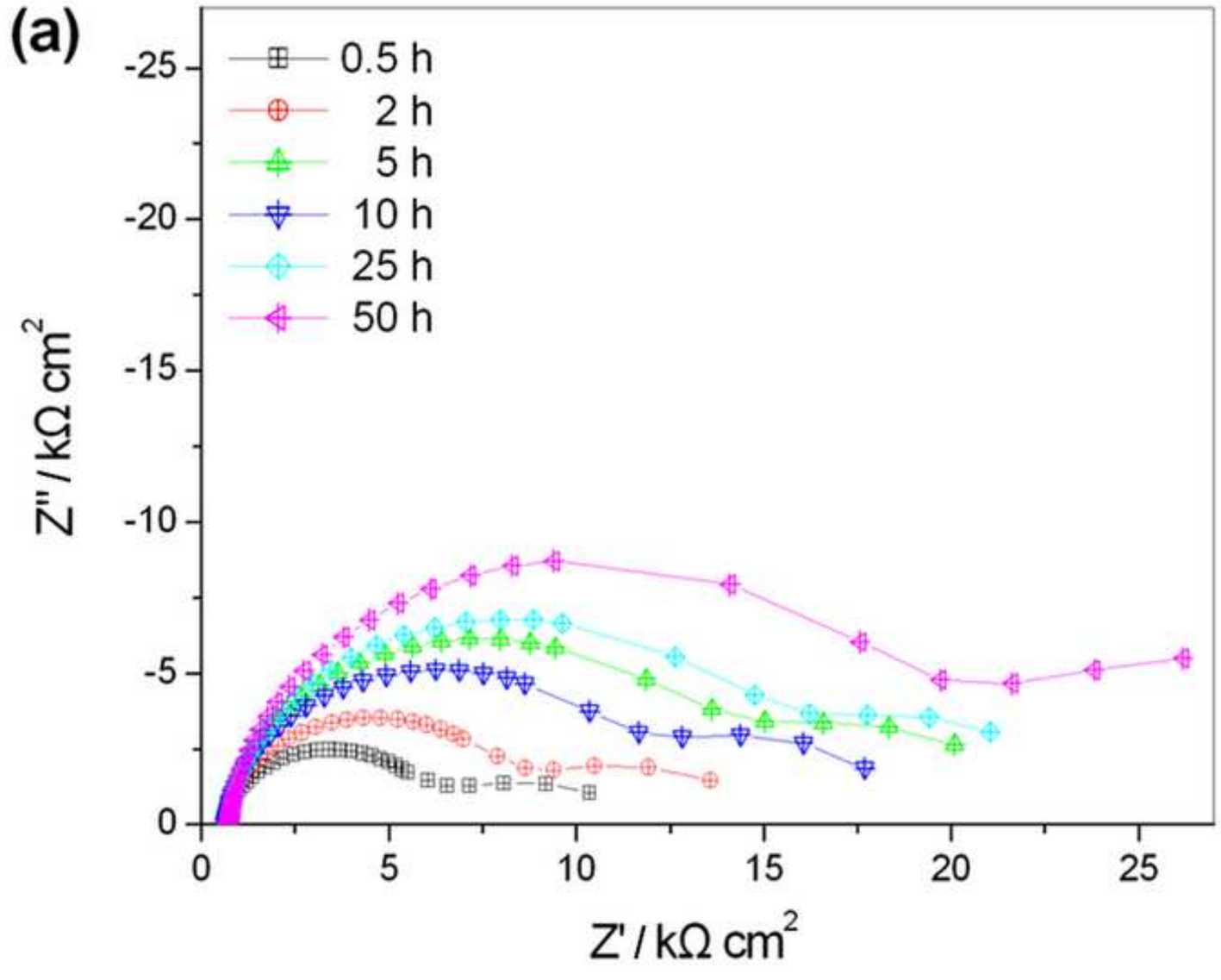

Figure 13b
Click here to download high resolution image

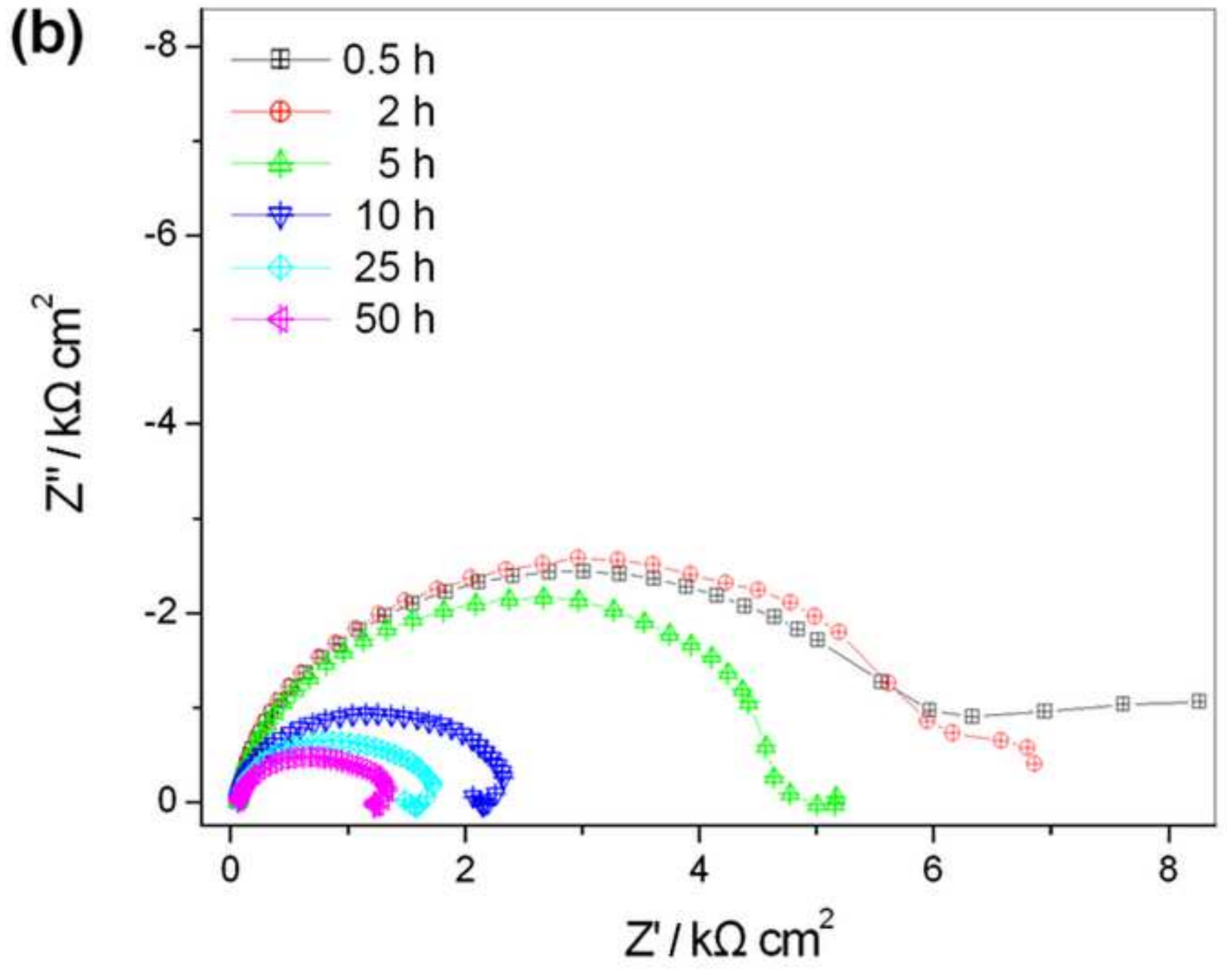

Tables

Table 1
Electrochemical parameters of Si-PEO coated specimens derived from polarisation tests in NaCl solutions of different chloride ion concentrations

Cl^- concentration (M)	E_{corr}/mV	i_{corr}/mA cm^{-2}	E_{bd}/mV
0.01	-1460 ± 30	(7.2 ± 3.0) × 10^{-6}	-685 ± 150
0.1	-1430 ± 25	(4.5 ± 2.5) × 10^{-6}	-1150 ± 40
0.5	-1430 ± 15	(2.0 ± 1.0) × 10^{-4}	—
1	-1440 ± 50	(3.7 ± 1.3) × 10^{-4}	—

Table 2
Electrochemical parameters of P-PEO coated specimens derived from polarisation tests in NaCl solutions of different chloride ion concentrations

Cl^- concentration (M)	E_{corr}/mV	i_{corr}/mA cm^{-2}	E_{bd}/mV
0.01	-1595 ± 40	(3.3 ± 1.0) × 10^{-5}	-1325 ± 15
0.1	-1555 ± 25	(6.8 ± 2.5) × 10^{-5}	-1390 ± 10
0.5	-1520 ± 5	(3.4 ± 0.3) × 10^{-4}	-1480 ± 10
1	-1490 ± 3	(3.6 ± 1.2) × 10^{-4}	—

Figure captions

Fig. 1. Surface and cross-section morphologies of PEO coatings formed in (a)-(b) silicate based electrolyte (Si-PEO) and (c)-(d) phosphate based electrolyte (P-PEO).

Fig. 2. Potentiodynamic polarisation plots of (a) Si-PEO and (b) P-PEO coated AM50 magnesium alloy specimens in NaCl solutions of different chloride ion concentrations (after 0.5 h of exposure).

Fig. 3. Electrochemical impedance behaviour (Nyquist plots) of (a) Si-PEO and (b) P-PEO coated specimens in 0.01 M NaCl solution (after different durations of exposure).

Fig. 4. Electrochemical impedance behaviour (Nyquist plots) of (a) Si-PEO and (b) P-PEO coated specimens in 0.1 M NaCl solution (after different durations of exposure).

Fig. 5. Electrochemical impedance behaviour (Nyquist plots) of (a) Si-PEO and (b) P-PEO coated specimens in 0.5 M NaCl solution (after different durations of exposure).

Fig. 6. Electrochemical impedance behaviour (Nyquist plots) of (a) Si-PEO and (b) P-PEO coated specimens in 1 M NaCl solution (after different durations of exposure).

Fig. 7. Macroscopic morphologies of corroded surface after 50h exposure/EIS testing in NaCl solutions of different chloride ion concentrations.
The dashed circles in the figure show the exposure area (0.5 cm^2) during corrosion test; the panes and letters label the specific SEM micrograph in Fig. 7.

Fig. 8. SEM micrographs of corroded surface after 50h immersion/EIS testing in NaCl solutions of different chloride ion concentrations.

Fig. 9. Schematic representation of a typical structure in Si-PEO coating and corresponding equivalent circuits employed to fit the EIS spectra at: (a) immersion stage with diffusion process; (b) immersion stage without diffusion process and (c) immersion stage after localized corrosion failure.

Fig. 10. Schematic representation of a typical structure in P-PEO coating and corresponding equivalent circuits employed to fit the EIS spectra at: (a) immersion stage before localized corrosion failure and (b) immersion stage after localized corrosion failure.

Fig. 11. The change of circuit elements (a) R_1 and (b) R_2 of Si-PEO coated specimen in equivalent circuits with immersion time in NaCl solutions of different chloride ion concentrations.

Fig. 12. The change of circuit elements (a) R_1 and (b) R_2 of P-PEO coated specimen in equivalent circuits with immersion time in NaCl solutions of different chloride ion concentrations.

Fig. 13. Electrochemical impedance behaviour (Nyquist plots) of uncoated AM50 magnesium alloy in (a) 0.01 M NaCl solution and (b) 0.1 M NaCl solution (after different durations of exposure).